Fachhochschule
Kaiserslautern
University of Applied Sciences

LMK
Landeszentrale für
Medien und Kommunikation
Rheinland-Pfalz

Prof. Dr.-Ing. Andreas Steil
Dipl.-Ing. (FH) Felix Schad
Dipl.-Ing. (FH) Martin Köhler

Summary Report

DRM$^+$-field trial Kaiserslautern, Germany
VHF-Band III
Trial period: January – May 2010

Date of issue: October 2011

Preface

This report on a field trial with DRM$^+$ at hand marks the closure of a set of field trials with DRM$^+$ in Kaiserslautern. The field trial this report deals with was performed in the time of january 2010 to the mid of june 2010 by the University of Applied Sciences Kaiserslautern. The obvious delay between the trial's execution and this report's delivery are due to staff and technical issues.

A trial of such a scope, empowering a huge effort to turn the city of Kaiserslautern and it's surrounding area into kind of a playground of two broadcast transmitters to enable the number of measurement and test-runs conducted, needs lots of material, know-how, time and – especially – the engagement of highly-motivated people. Lots of tasks, too much to be be tackled by the authors alone: There were lots of people and organizations involved by either personal, material (or even both) support. First and foremost, our gratitude goes to the Landeszentrale für Medien und Kommunikation (LMK) Rheinland-Pfalz (media authority of the state of Rhineland-Palatinate), for a long and intense cooperation regarding the digitisation of terrestial broadcasting services.

The authors would like to use the opportunity to express their thanks to *ALL* people involved. Special thanks go to M.Sc. Michael Feilen, the Federal Network Agency of Germany, the Südwestrundfunk (SWR), Co. Hans H. Plisch, the Fraunhofer IIS and the Rohde & Schwarz Vertriebs GmbH. The engagement, support and trust given to the project by them is one of the key factors for it's continous success.
Furthermore, we'd like to express our gratitude to the companies and institutions for their support and advice: Robert Bosch GmbH, Deutsche Flugsicherung GmbH (DFS), Dolby Germany GmbH, ARD.ZDF medienakademie, Ruoss AG, LfK Baden-Württemberg, Kathrein, Spinner, BMW, Media Broadcast GmbH, PURE digital, NP Technologies Inc., Institut für Kommunikationstechnik der Universität Hannover, ATMEL Germany GmbH and Mr. Kuhn.
Please note that this enumeration implies no weighting at all. The authors desperatly hope that no one has been forgotten.

Although this report marks the shutdown of a major center of DRM$^+$-activities in Germany and although it is not as elaborate as the previous publications – the DRM-System's future is still open and eager for (your?!) contribution.

Have fun reading!

Munich / Kaiserslautern, in the autumn of 2011

Andreas Steil Felix Schad Martin Köhler

Please note that Mr. Felix Schad's affilitation has changed in the meantime. He is now with the German Federeal Network Agency. The present report can be seen as his final contribution to the DRM$^+$ topic by concluding the work he has done at the University of Applied Sciences in Kaiserslautern. Please note that, therefore, the content of this document is in no way correlated with the author's current affliliation at all.

Contents

1 Executive summary

The field trial described in this report at hand has shown that the operation of DRM$^+$ in the VHF Band III is possible in a real-world scenario.
The trial's outcome can be summarized as follows:

- DRM$^+$ operation in a real-world scenario is possible, even with the use of modified DAB-receiving frontends.
- Measurements in a mobile and stationary scenario reveal a good coverage performance that matches quite well with preliminary frequency planning excercises based on the laboratory values.
- Adjacent-channel interference was barley to simulate in this trial comprehensively. The impressions gained tend to harden the protection ratios evaluated prior to the field-operation.
- Co-channel interference is controlable. The results tend to confirm the protection ratios evaluated prior to the field-operation.
- Speed issues due to the increased doppler shift in this frequency range as compared to band II exist, but have shown to be much more promising in the local terrain situation as seen in [Köh10].

The trial shows that DRM$^+$-operation in this frequency band is possible and that it can coexist compatible and complement the digital audio broadcast solution established already in this frequency range.

2 Introduction

2.1 Starting position

DRM$^+$ has got quite a kind of history in Kaiserslautern. The pace has been set by theoretical considerations [Ber05] that settled the basic idea, showed up the key parameters and finally caught some attention on the international working parties of the DRM consortium. The still nowadays evolving work of M.Sc. Feilen in creating his software-based transmitter 'Spark' [Fei05] capable of creating the DRM-baseband for the Modes A-E including a convenient content-management pushed the idea further and led to first steps in Kaiserslautern towards a real transmitter [Sch07]. Due to the growing interest and continued support by the state media authority of Rhineland-Palatinate (LMK), an experimental transmitter was built. Preliminary, large-scale measurements regarding the interference potential of DRM$^+$ into the FM-broadcast service and adjacent services created a basis for the first experimental frequency assignments for DRM$^+$ among other candidates for the digitization of the VHF band II [HSE07]. Following this, Kaiserslautern was the scene for two elaborate field trials incorporating a small-scale, but nonetheless real-world scenario for the investigation of the interference potential of DRM$^+$ in the field [SS08]. Furthermore, the first realtime transmission of broadcast material over the 'DRM$^+$-channel' was realized and proven to an international audience. The second trial dealt with the performance of DRM$^+$in the laboratory and in the field. For the first time, protection ratios for realistic DRM$^+$-receivers were determined. Once again, a field trial was set up using an DRM$^+$-transmitter and an FM-transmitter on two sites in Kaiserlautern. Not only the performance of the system was investigated, also the robustness to interference has been a major part of that certain trial. Along it's way, major aspects regarding monitoring of DRM$^+$-stations were identified and taken care of by the creation of a dedicated live-monitoring system. Procedures of comparison and enhancement of DRM$^+$-radio network planning methods were proposed and conducted [SSK09].

Not all of the work items dealt with so far are reflected by this brief history, but during time it became more and more obvious that for different reasons DRM$^+$ (among other candidates for the digitization of VHF band II) has one key problem to overcome in ITU-region I: the simple fact that the band is plain full - not just only in a sense of coordination procedures. Thus, the idea of a 'step forward' onward to Band III came up for various and obvious reasons as discussed in [SLSK08]. Not only the price and broadcasting opportunities for smaller, regional stations without the need for large, state- or nationwide allocations are more attractive with an DRM$^+$-transmitter, also the frequency allocations on a national and European scale are easier when thinking about the availability of spectrum.

Thus, work started over to set up a transmitter capable of band III-operation. Soon after, in the october of 2009, a full fledged transmission chain was ready and proved it's operational state. Once again, protection ratios into and against the DAB-system (the 'big brother' of DRM in the family of digital audio broadcasting standards) were measured. Realtime hardware simulations offered the first real-world information about the system's performance in this frequency range that is out of the design's scope for DRM Mode E, namely the specified upper frequency border of 174 MHz as defined in [Ins09]. The results were positive and encouraged the set-up of the field trial at hand, cf. [Köh10].

2.2 Set goals

Following terms shall be investigated in this trial regarding DRM$^+$in Band III:

- Proof that the laboratory setup can be used sucessfully in an real world environment.
- Assessment of real-world performance.

2.3 Contents overview

This document is organized in a more loose way than the reports about the Kaiserslautern trial's before. It is to be read as a loose follow-up of several investigations due to periods of breaks during the trial for changes on the transmitters and device availability schedules, leading to test drives used only for cross-checks, measurement repetition and so on to ensure that previous results still were valid / reproduceable (e.g. weather influences, transmitter hardware changes). Furthermore, if a certain measurement data evaluation is needed to explain things in a certain trial's phase relying on data recorded earlier, then the evaluation will show up at the spot where it is actually needed and not in the phase were it was recorded. This helps to keep the information needed at right the place where they are actually of interest, circumventing the need for the reader to jump back and forth in the document.
This document is organized as follows:

Chapter 3 explains the trial's setup, document's the transmitter's data and setup and explains the concepts and measurement methods applied. Information about the measurement route are given, along with an overview of the geographical situation in the target area.

Chapter 4 documents the first period of the trial. The relevant parameters of that phase are denoted there. The measured fieldstrength distribution from the transmitters are shown here. During the trial, the powers and frequencies of the transmitters will be altered, but the general propagation path's won't, so one set of figures like these is sufficent.

Chapter 5 documents the seconds trial's perdiod. The relevant parameters of that phase are denoted there. The evaluations shown in this chapter focus on the interference from DRM$^+$ into the DAB service.

Chapter 6 focussed on the interference of the DRM$^+$-service by DAB.

Chapter 7 deals with measurements done in a stationary reception scenario, independent trial's current phase.

Chapter 8 is an extensive attempt to extract information about surplus levels needed for radio network planning for the mobile reception scenario from the measured data.

Chapter 9 reports about a test drive aiming to assess the performance of the DRM$^+$-system in regards of high velocities.

Chapter 10 concludes the report with a roundup of the whole trial.

3 Trial's setup, applied principles and general information

3.1 Transmitters

The site data of the transmitters used are listed in table tab. 3.1. A graphical overview of the transmitter site's closer vicinity, their relative position to each other and the antenna patterns is given in fig. 3.4.

Throughout the rest of this document, the transmitters are to be referenced by their inidivial shorthands, namely:

- **TX FH (site: 'Am Kaiserberg, FH')**
- **TX RB (site: 'Rotenberg')**

TX FH was realized using the schematic sketched in [Köh10, S. 61]. Furthermore, thanks the Hans H. Plisch company, the module 'ULE820' could be used as a final amplifier. Output filtering was achievied using a DAB-maskfilter supplied by Spinner, cf. [Köh10, S. 99 ff.]. Thanks to the dedication of Plisch, a power boost from 90 W to 180 W was achievied by the start of May due to the dedication of a pair of combiners and another ULE820.

TX RB was realized by a demo-license of Fraunhofer's DAB / DAB$^+$-Contentserver and lend Rohde&-Schwarz DAB-Transmitter SLA8000. The SLA8000 was replaced at the end of May by a Plisch-Transmitter TDA3503S. Both transmitters were capable of accepting DAB and DAB$^+$-streams. Output filtering was achievied using a DAB-maskfilter supplied by Spinner. The transmitter-site, the antenna (cf. fig. 3.1) and the manpower for it's mounting was provided by the friendly support of the SWR.

	TX FH	TX RB
Location Position (WGS-84; decimal degree) Position (GK3; Easting / Northing	'Am Kaiserberg' (emperor's hill) 49,4506N;7,76316E 3410383;5480035 260 m a.SL., 30 m a.SL.	'Rotenberg' 49,459579N;7,771260E 3410954;5481026 310 m a.SL, 50 m a.SL.
Modulation	DRM$^+$	DAB / DAB$^+$
Channel	10B or 10C	10B
max. ERP	90 W since May 2010: 180 W	180 W
Antenna's radioation pattern	ND	D, 5-element Yagi
Antenna's main direction	N.A.	260°
Polarization	vertical	vertical

Tab. 3.1: Site-data of the trial's transmitters; GK3: Gauss-Krüger, 3rd Strip

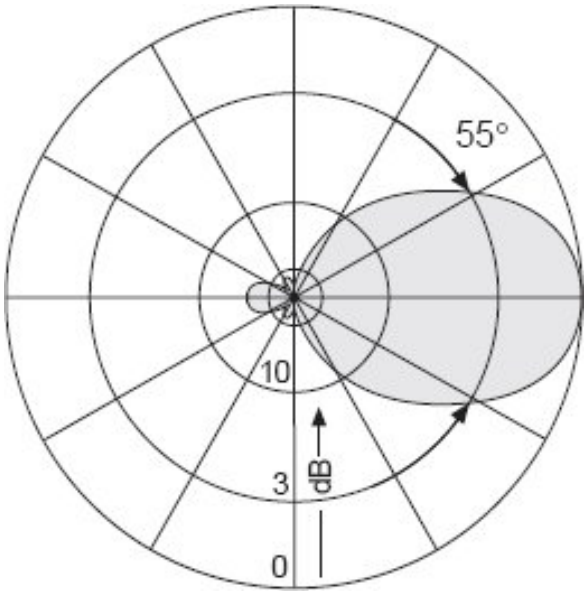

Fig. 3.1: Left: Antenna pattern of TX RB (horizontal polarization plane)

The output spectrum of TX FH is shown in fig. 3.2, measured at a directional coupler mounted immediately after the final output filter (coupling losses are incorporated into the levels values shown on the figure). A total output power of 90 W is radiated when the cable loss from the measurement point to the antenna's insertion point is considered.

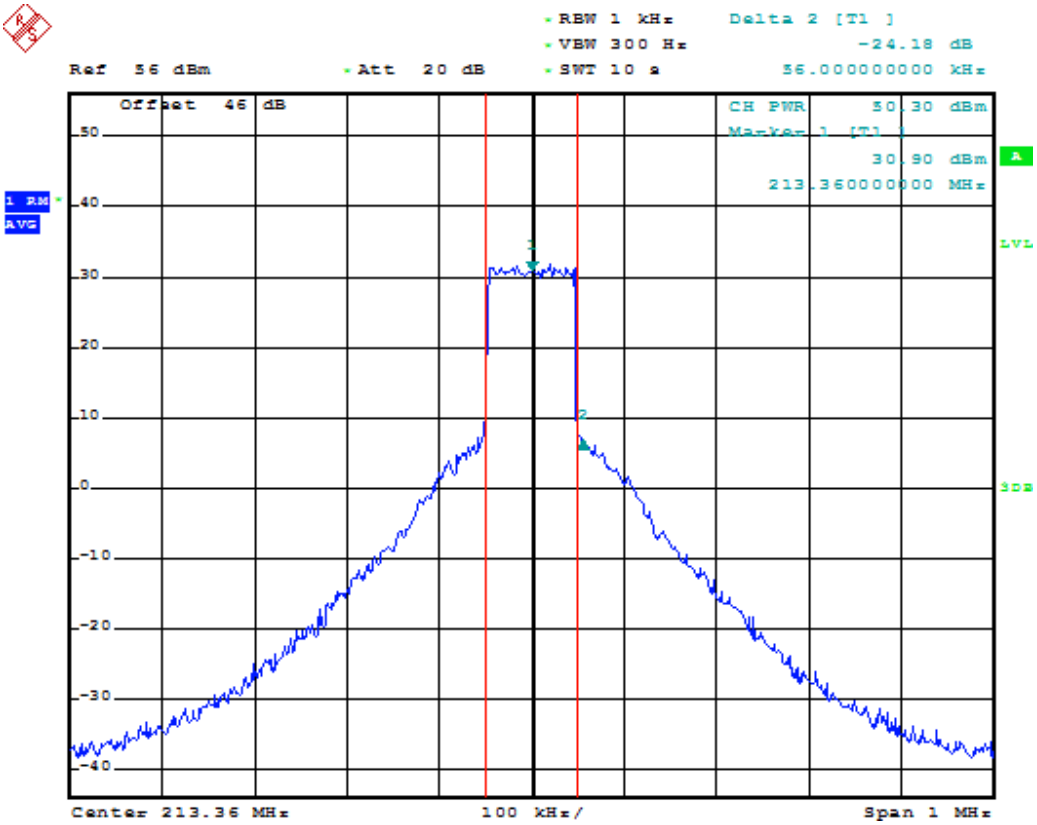

Fig. 3.2: Output spectrum of TX FH

The photos in fig. 3.3 show some impressions of the trial.

Fig. 3.4 shows a map of the Kaiserslautern area where the trial took place. In the background, a relief area of the topographical features is displayed. The transmitter sites are marked, along with their respective antenna patterns. Due to the directional nature of TX RB's antenna, blue circles

indicate the 0 dB, 3 dB and 10 dB sections fitted onto the map's scale and antennas direction, as they can be found in fig. 3.1. Furthermore, the diamonds mark the spots where stationary measurements took place.

Fig. 3.3: Left: Self-made groundplane antenna of TX FH (foreground), watching over to TX RB (background); Right: Power amplifier and filter installation of TX FH using Plisch-equiqment for the radiation of 180 W.

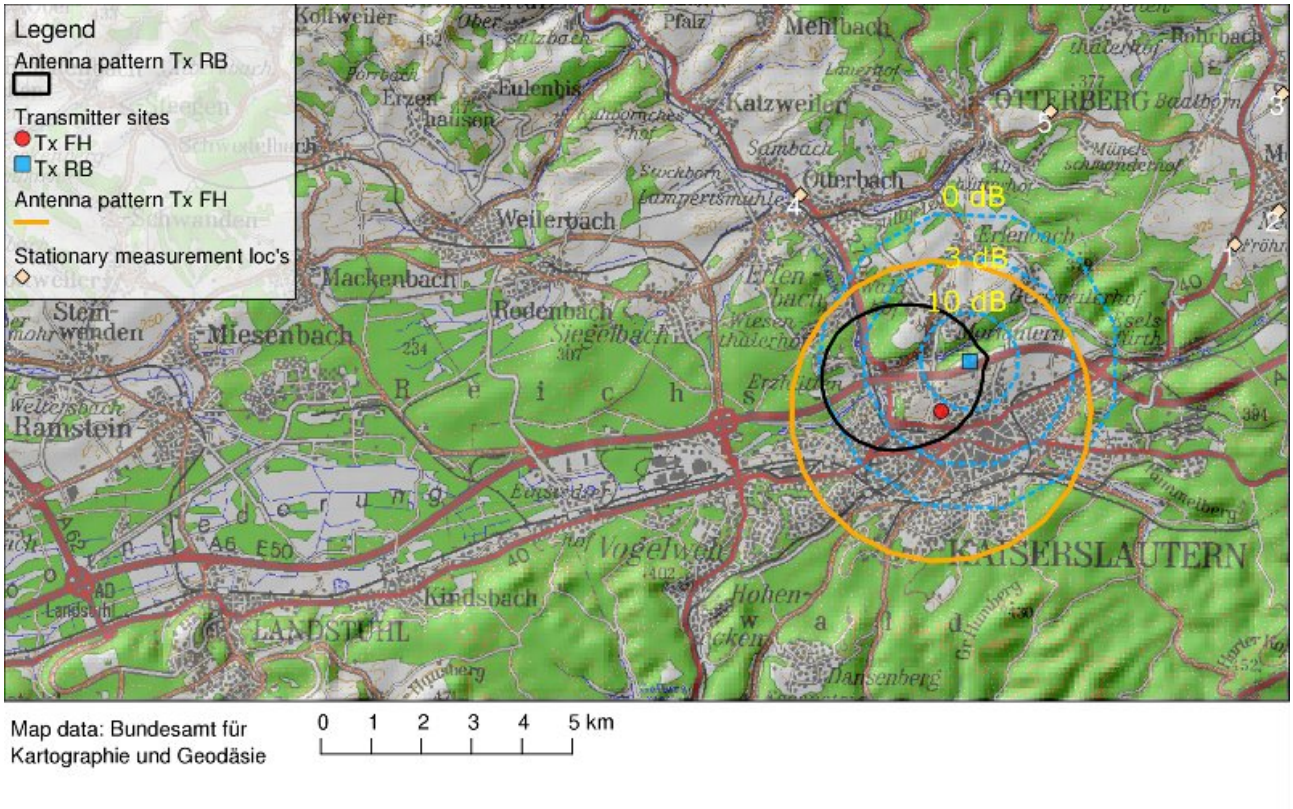

Fig. 3.4: Location and antenna patterns of the trial's transmitters in Kaiserslautern, Germany

Both transmitters were controllabe via an Internet-based access system, enabling control of the transmitters operation and the multiplex's contents and encoding. Both DAB-transmitters incl. the contentserver offered this option; for the maching running the Spark software, a special access route was created. For the transmitter itself, a little wxPython based script shown in fig. 3.5 was used to control the RF-side, i.e. switching the transmitter's output on / off and controlling the transmit power in 1 dB-steps.

3.2 Receivers

The receivers used are the ones that were engineered, described and measured in [Köh10]. The DRM$^+$-receivers were functional since the end of october 2009. Some aspects that are to be emphasized additional are as follows:

DRM$^+$-Rx1: a receiver based on Maxim's frontend MAX2172 featuring a low IF of approx. 2 MHz. The configuration for the trial was set in such a way that the tunable IF-Filter (right before the Perseus' input) was operated as a small-band filter (i.e. 180 kHz) as a compromise between DRM$^+$'s narrow-band channel width and an increased noise figure due to the filter's higher insertions loss (compared with the built-in DAB-Rx-Filter).

DRM$^+$-Rx2: Rx2 is a modified DAB-demonstration receiver used in the automotive industry. The high IF of about 39 MHz was tapped using a matching balun. The tap was connected to the Perseus, thus enabling the receiver to be operated as a DAB- and DRM$^+$-receiver in parallel. The IF-filter was kept as the receiver's already built-in DAB-Filter with a 3 dB-bandwidth of 1.5 MHz. The overal noise figure of this receiver his lower than Rx1's noise figure. This receiver is the standard-receiver for DRM$^+$in this campaign, unless noted otherwise.

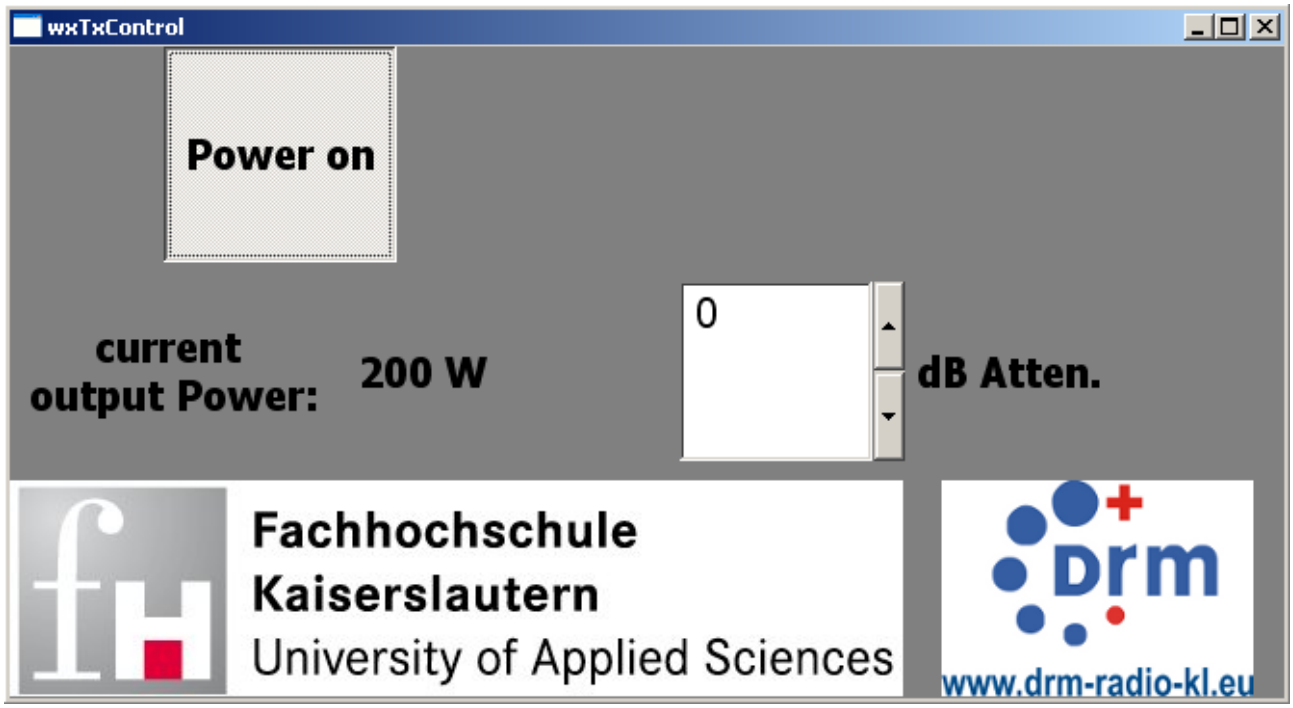

Fig. 3.5: Control interface of TX FH

After the IF-section of Rx1 and Rx2, the receivers fed the signal to the Perseus-receiver [Mic]. Conceptually, the Perseus consists of an ADC[1] with an integrated DDC[2]. It delivers the digital baseband-samples via USB to a computer running Mr. Feilen's ratemonkey-software. The samples are converted from a wordlength of 3-byte wordlength with a sampling rate of 250 ksamples/s to 192 ksamples/s with a wordlength of 2 byte. The resulting stream is fed via a LAN-interface to Fraunhofer's DRM$^+$-decoder. Thus, the same DRM$^+$-decoding and monitoring equiqment was usable for both receivers available. The RSCI-/MDI-stream generated by the decoder was distributable via the LAN-interface to a single listener or (via an selfmade python-script) to several listeners, e.g. audio-decoder and multimedia-decoder.

For DAB-reception, the following devices already illustrated in [Köh10] were used:

Rx2: Rx2 is the same as Rx2 used for DRM$^+$-reception. Monitoring of DAB-decoding is only possible via recording it's analogue audio output. Indicators of the reception level and the estimated DAB-error rate *before viterbi-decoding* are available. A distinction of Rx2's operational mode is not made during this report, for the chosen mode should usually be clear from the report's context.

Rx3: Pure Evoke Avanti, DAB$^+$-capable. Monitoring of DAB-decoding is only possible via recording it's audio output.

Rx4: VAD UEB 400 USB. A DAB-measurement receiver, built from hardware comparable to Rx2. Monitoring of the DAB-decoder's states is capable by the use of a self-made software tool. Since Rx4 is a dedicated measurement receiver with the possibility of accessing many information relevant to the whole DAB-reception process from the RF-side to audio-decoding. This property made Rx4 the premier choice for mobile measurements. Unfortunatley, Rx4 isn't capable to deal with DAB$^+$.

The following table 3.2 summarizes the key measures of the receivers used for DRM$^+$ bzw. DAB/DAB$^+$, based on the measurements done for [Köh10].

[1] Analogue to digital converter
[2] Digital downconverter

	Rx1		Rx2	
Subcarrier modulation	4-QAM	16-QAM	4-QAM	16-QAM
MDS / dBm	-112,2	-106,2	-117,2	-112,2
IF 3 dB-BW /khz	133		1527	

Tab. 3.2: Key data of the DRM$^+$-receivers used in the trial

Rx-Number	Rx-Name	MDS/ dBm	DAB$^+$-capable
Rx3	Avanti	-98	$\surd$
Rx2	Unkown manufacturer	-101	–
Rx4	VAD	-101	–

Tab. 3.3: Key data of the DAB-DAB$^+$-receivers used in the trial

3.3 Parameter of the emitted multiplexes

3.3.1 DRM$^+$

For DRM$^+$, the transmitted signal consisted of one audio stream and one PRBS stream.
As in the trials before, two variants of the MSC-modulation depth were tested for DRM$^+$, namely one 4-QAM-variant and one 16-QAM-variant. For the 4-QAM-variant, the SDC protection level (viterbi coder) was set to 0.25, the MSC protection level was set to 0.4. For the 16-QAM-variant, the SDC protection level was set to 0.25, the MSC protection level was set to 0.33.

3.3.2 DAB / DAB$^+$

For the DAB / DAB$^+$-multiplex, there existed one stream in the whole multiplex using about 96 kBits/s for the audio stream both for DAB and for DAB$^+$.

3.4 Measurement methods and evaluation strategies used

The most common type of measurement in this campaign covered the mobile reception scenario. As shown in the following chapters, several situations were constructed using different settings of TX FH and TX RB. For each scenario, a measurement run was performed using a measurement van.

For DRM$^+$, the Universities measurement van was equipped with the setup developed for [SSK09]: a $\lambda/4$-dipole is mounted on the van's rooftop. A distance-pulse-counter is attached to one of the rear wheels, set up such that one pulse is emitted every 0.8λ passed [Lee93]. The antenna signal is split using a 3 dB-splitter. One path is routed to a receiver, the other one is routed to a spectrum analyzer. The receiver is connected to a dedicated measurement software via LAN, the analyzer is connected to the measurement software via an IEC-Bus. The analyzer is set in such a way, that ever distance pulse triggers a sweep in zero span over a length of roughly 30 ms, setting a maximum speed of 120 km/s. The analyzer's bandwidth is set to a 100 kHz-channel filter. The trace is taken with an rms-detector. The RMS-power over the whole trace is taken as the power at the receiver's input in the receiving window. This value is sent to the computer upon completion of the trace. This triggers the storage of values like the current BER, MER, position as reported by a GPS-receiver, etc. onto a measurement file.

For DAB, the same antenna was used. The measurement receiver 'VAD UEB 400 USB' was used for level measurements, decoding and reception status information. An adapter software was created to 'connect' the DAB-receiver to the existing measurement software. To keep the antenna conditions the same for DAB than in the DRM$^+$case, the splitter was kept, but one port was terminated using a 50 Ω-resistor. Anything else, especially the distance-pulse-counter mimic was kept.

Upon completition of a measurement run, the acquired positional data were equalized to enforce a distance of 0.8λ between sucessive samples as demonstrated in [SSK09], using the a-priori-knowlegde that the samples are enforced to be taken upon a trigger from the distance-pulse-counter. Thus, the equalization process decouples the samples position which are bound the the GPS-receiver's system rate and shifts the samples position to the true vehicle's position.
Afterwards, the standard result evaluation as described in [SSK09] is performed to make the sample data comparable to rasterized data as it is usually found in radio network planning. The planning / measurement rasters were chosen to a size of $100\,\mathrm{m} \times 100\,\mathrm{m}$. Following strategies / steps were used to conduct this conversion:

- for power levels, the raster pixel's value is the median of the power levels that occured on those samples that fall into the raster area.
- for the raw, instantenous bit-error-ratios collected from the DRM$^+$-receiver, the third quartile of the bit-error-ratios of those samples that fall into the raster area is deteremined to make up the raster pixel's value. As already stated in [SSK09], uninterfered audio decoding is possible if this median value is above the threshold of $1 \cdot 10^{-4}$. Figures of measurement drives containing these numbers as a basis will show the areas with uninterfered audio decoding as green pixels, red otherwise.
- in the case of DAB, the receiver was able to supply p.e. the number of erroneus and thus muted audio frames, if the receiver was able to syncronize with the DAB-stream / the embedded, selected audio stream and the received signal power. The audio is regarded as error-free, if
  1. there are up to 10 erroneus audio scale factors,
  2. the receiver is synchronized to the audio stream,
  3. the audio decocder has not muted a single audio frame.

  The arbitrary number of up to 10 scale-factor-errors was chosen after a few test drives and test-evaluations, to match the perceived impression of the reception process with the data represented by the measured value representing the 'audio decoding ok'-flag.

As already mentioned above, care has to be taken to get a representative value for a certain region during the rasterization process. For this, several possibilites for the aggregation from the samples to the raster-level were taken into account. An example is shown in fig. 3.6. In this demonstration figure, the 'audio decoding ok'-flag as mentioned above was evaluated as it happened to the momentary bit-error-rate for DRM$^+$ above: the samples that fell into an area of a raster pixel were aggregated and rated: when the 3rd quartile (upper left), median (upper right), 9th percentile (lower left) indicated that the percentage of 'audio decoding ok'-flags are positive, then the pixels color turns red ('DAB Audio ok'), yellow if it isn't. Thus, red spots in this figure indicate 'audio reception ok', yellow spots 'audio reception fails'. Finally, the lower right picture shows the variance in the 'audio decoding ok'-flag in the raster areas of interest. This portion of the picture in conjunction with the colormap indicates that the turnover from 'good reception' to 'bad/failing reception' comes fast and hard – areas, where there are many sampling points marked 'good' and as many points that are marked 'bad' are not present. Thus, the choice between the median, 3rd quartile or any higher percentage is not very sensitive regarding a binary rating between 'reception ok' and 'reception not ok'. Thus, the 3rd quartile was chosen as a standard evaluation strategy, keeping consistend with the way the DRM$^+$-decoding state is represented. Furthermore, the images match the DAB-audio performance percieved during the drives along the route.

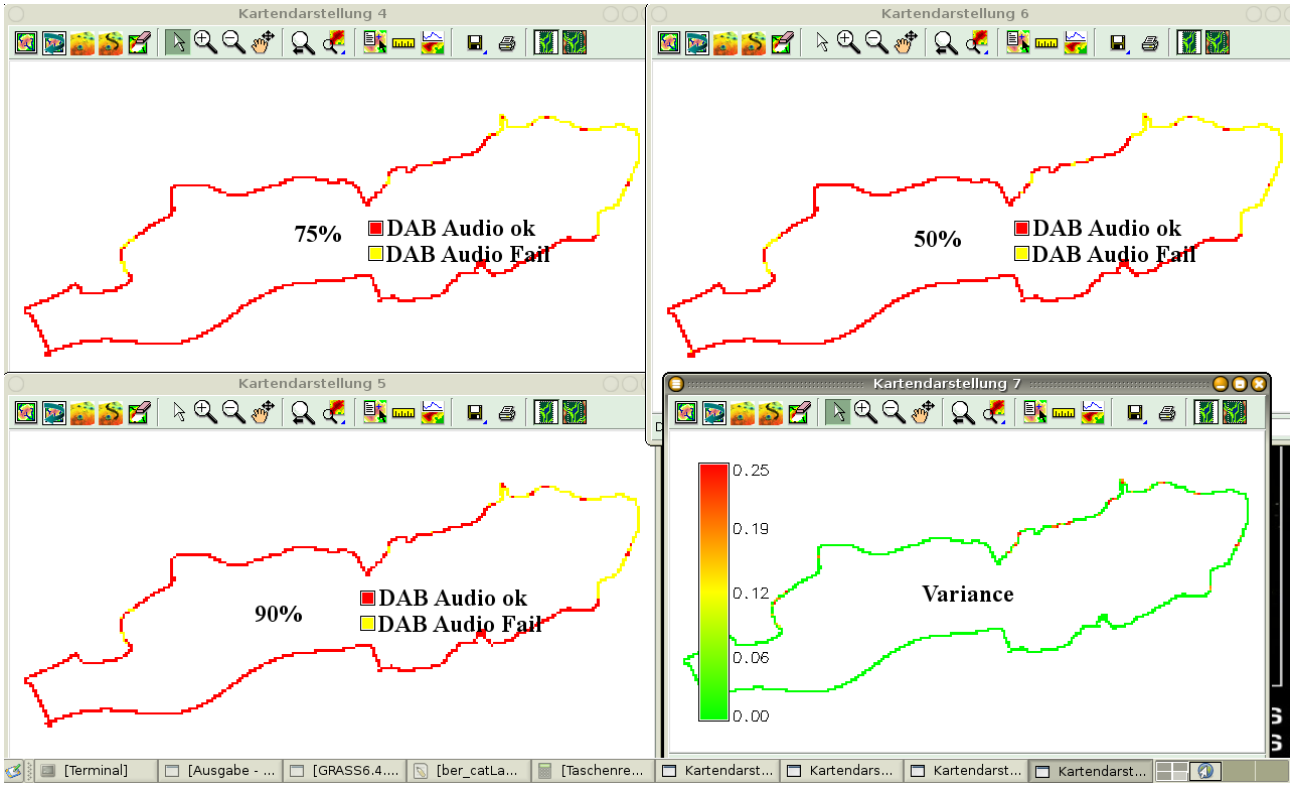

Fig. 3.6: Comparison of the impact of several resampling-streategies during the rasterization process

3.5 Description of the measurement route

The route for mobile measurements was chosen to meet following requirements and is shown in 3.7:

- passage of both transmitters, to get high levels from both systems.
- passage of regions where each of the transmitters dominate in their power levels or are roughly equal.
- passage of rural, suburban[3] and hilly regions.
- passage with different speed profiles: city, living area, freeway, country lanes, federal highways.

[3]Due to Kaiserslautern's size and building structure, this scenario yield urban features quite seldom

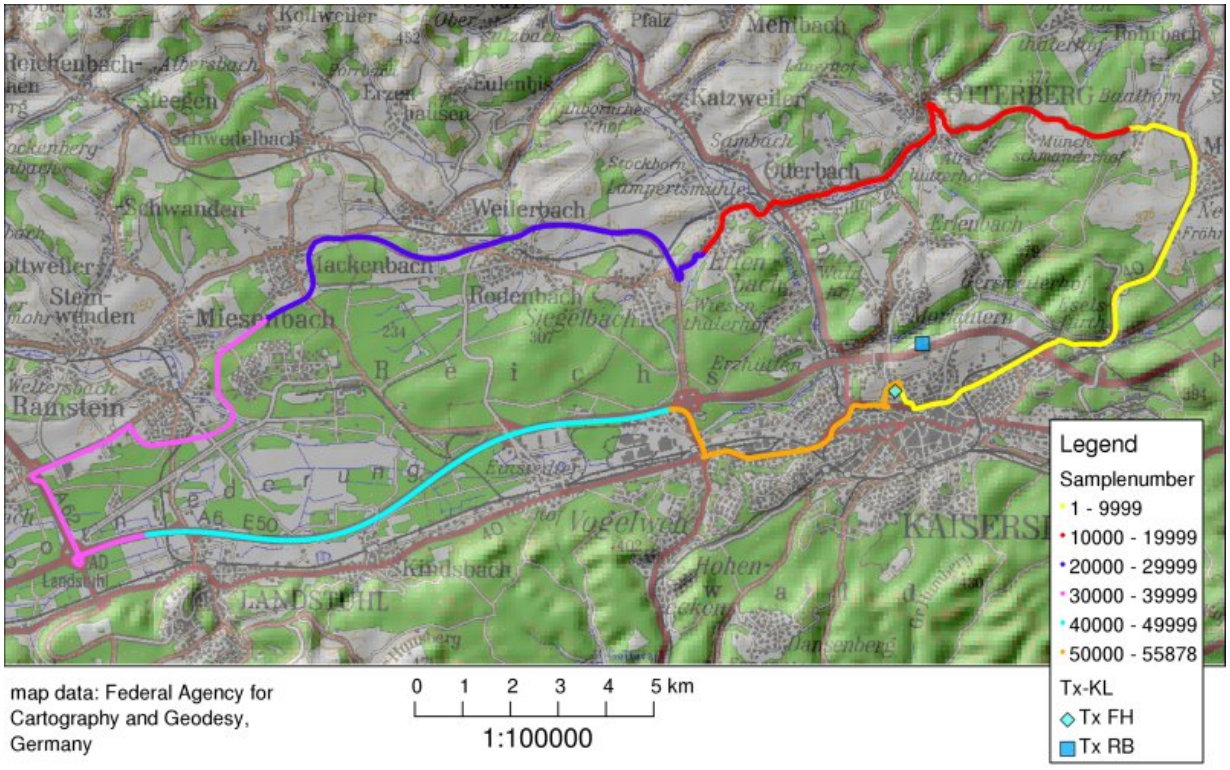

Fig. 3.7: Overview of the measurement route. The sample number regions are shown as a reference for figures used later

An overview map of the towns around the measurement route (shown in purple) is shown in fig. 3.9. That figure is assorted with fig. 3.8. Both maps scales are equal for the ease of comparison. The topographic map is meant to give the reader an impression of the topographical situation of the region, which spans mainly the Kaiserslautern basin, the west-palatinite hills and the marsh of Landstuhl. The color scale in fig. 3.8 represents the height; the white circles mark the locations of the transmitters involved. While TX RB is located on a cliff along the speedway, TX FH resides on a less exposed spot, but still is slightly higher than the city. This is a natural restriction, for the University's campus hasn't been chosen to host a broadcast transmitter site. As can be seen on the following figures 3.10 and 3.11, the consequences for the radio link in terms of line of sight conditions are not negligible.

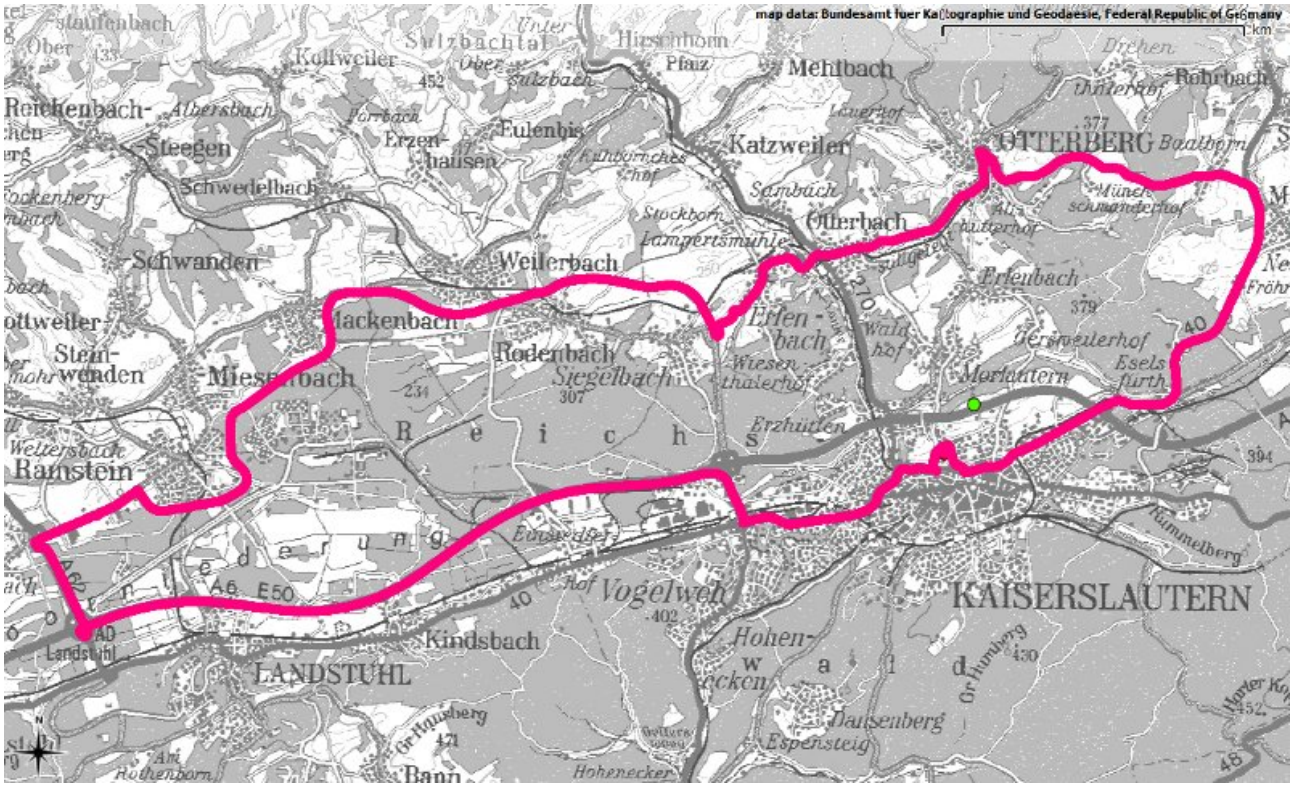

Fig. 3.9: Overview map showing the measurement route and the town names in the Kaiserslautern region

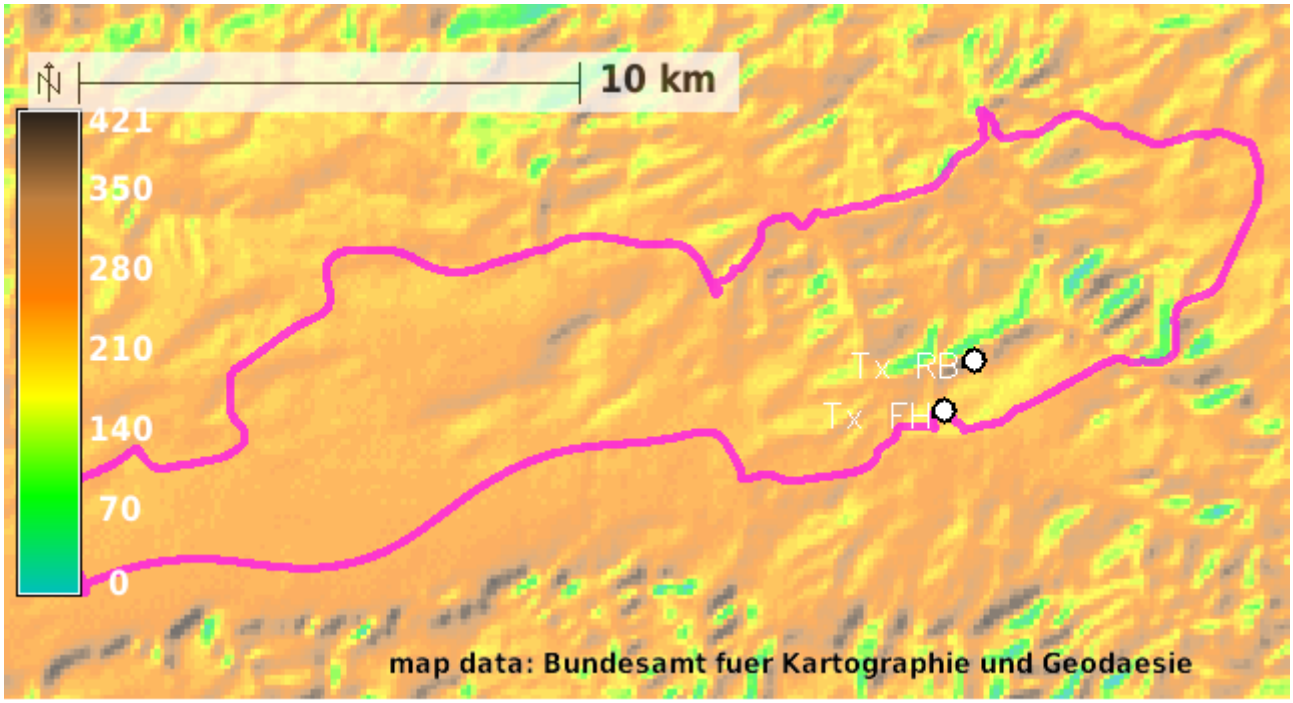

Fig. 3.8: Topographic overview map of the trial's region. Only the rectangle that entangles the measurement route is colored; the color-scale marks the height.

[H] The route starts at the campus of the University of Applied Sciences, right next to TX FH. It goes right down the emperor's hill to the outskirts of Kaiserslautern downtown and leads outwards to a hilly region with direction Mehlingen. During this passage, the back lobe of TX RB's antenna is aimed. Furthermore, the level of TX FH drops, since the line of sight is cut (yellow route section). In

the red route section, both transmitters are shaded due to the terrain. TX RB's back lobe diminishes as the route continues to the blue section. Although the terrain's roughness starts to get smoother and both transmitters are partially more visible to the reception antenna, the levels are still low. Reflection path's get even shorter, due to the road is partially embraced (e.g. in the region around Mackenbach) by hills for reducing motorway noise; they are not wider apart than about two lanes and a little bit higher than a truck. The purple section is the one that is most distant from all transmitters, but is located in TX RB's main beam. The route leads to the freeway, directing back to Kaiserslautern. Both transmitters get closer while driving through the marshes of Landstuhl. Finally, the routes white section marks the point where the freeway is left. The industrial regions of Einsiedlerhof pass along the military buildings along the roadside to Kaiserslautern. After the passage of light industrial and living quarters, the route's end at TX FH is reached.

As a further reference, the LOS conditions and indication of the number of diffractions bends as perceived by an antenna in the measurement van's height are shown for both transmitters in the following fig.'s 3.10 and 3.11. Comparison of both figures reveals the impact of the low antenna height for TX FH and also justifies the main lobe's direction chosen for TX RB. Furthermore, it becomes evident at the first sight that an essential coverage limit esp. for TX FH is the ratio of low antenna height and the terrain's roughness, which is a distinctive feature of that region. From a receiver's point of view, this terrain is tough due to the roughness (fast level shifts) compared to the narrow aisles paired along with longer reflection path's receiverd from the higher southern hills.

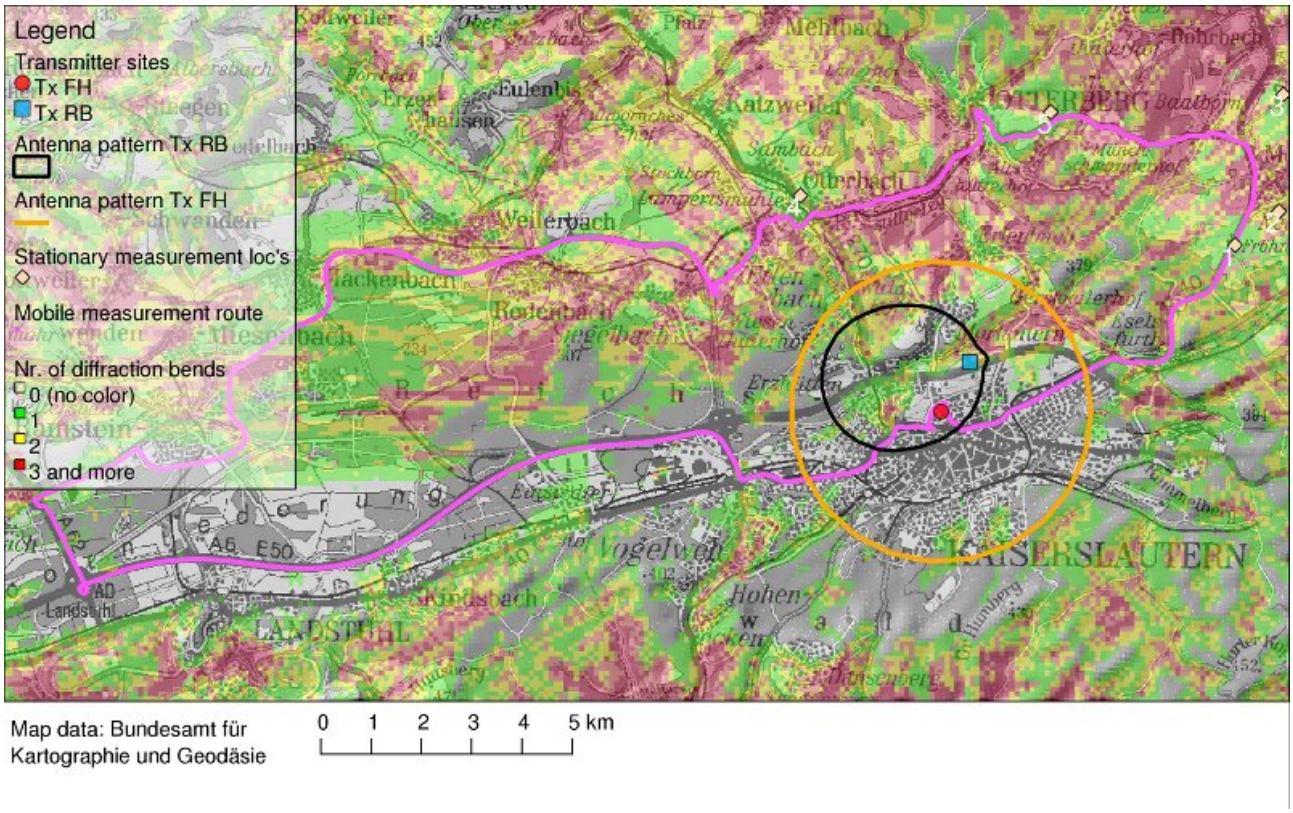

Fig. 3.10: LOS conditions / number of diffraction bends for TX FH

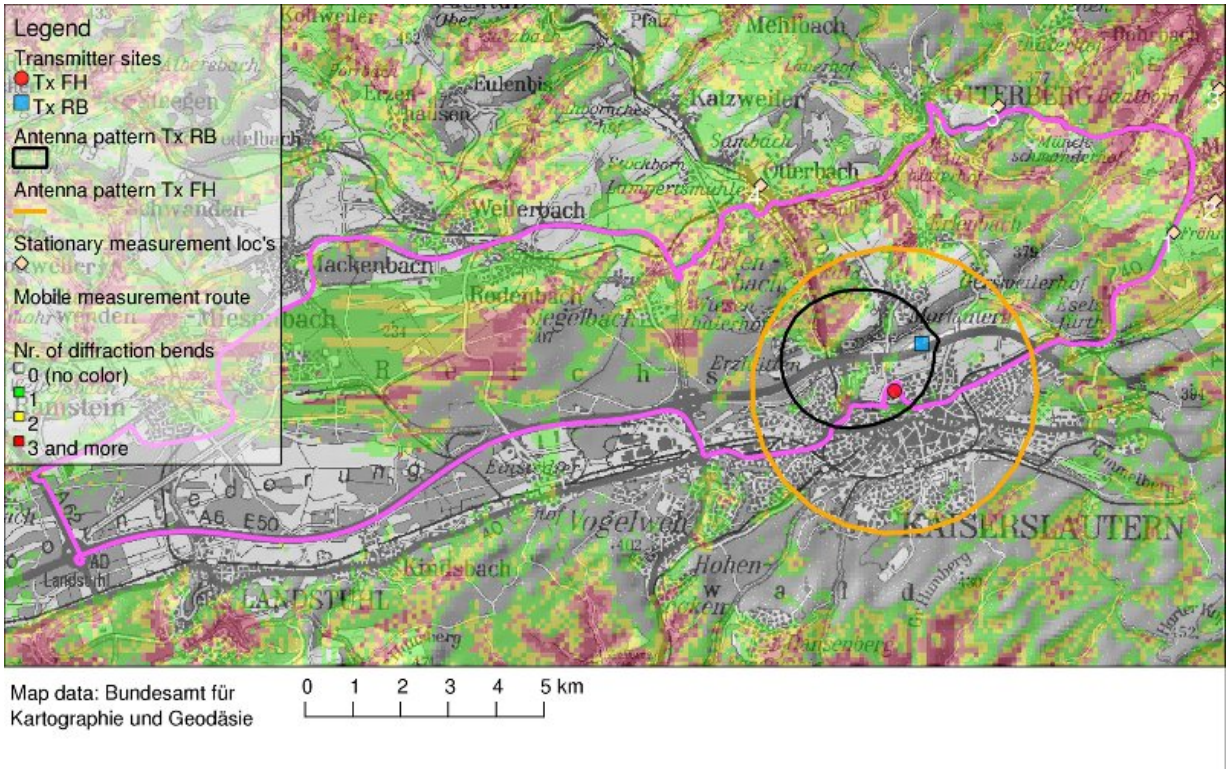

Fig. 3.11: LOS conditions / number of diffraction bends for TX RB

The following figure 3.12 shows the relative height between the transmitters and the receiver along the measurement route in red / green (left ordinate). A positive height indicates that the receiving antenna is below the transmitting antenna. A negative height indicates that the receiving antenna is higher than the transmitting antenna. This plot is meant to give an impression about the route's height profile and the good line of sight conditions of TX RB.
The blue / purple plots show the distance from the reception location to the transmitter locations. The corresponding distance measures are shown on the right hand ordiante.

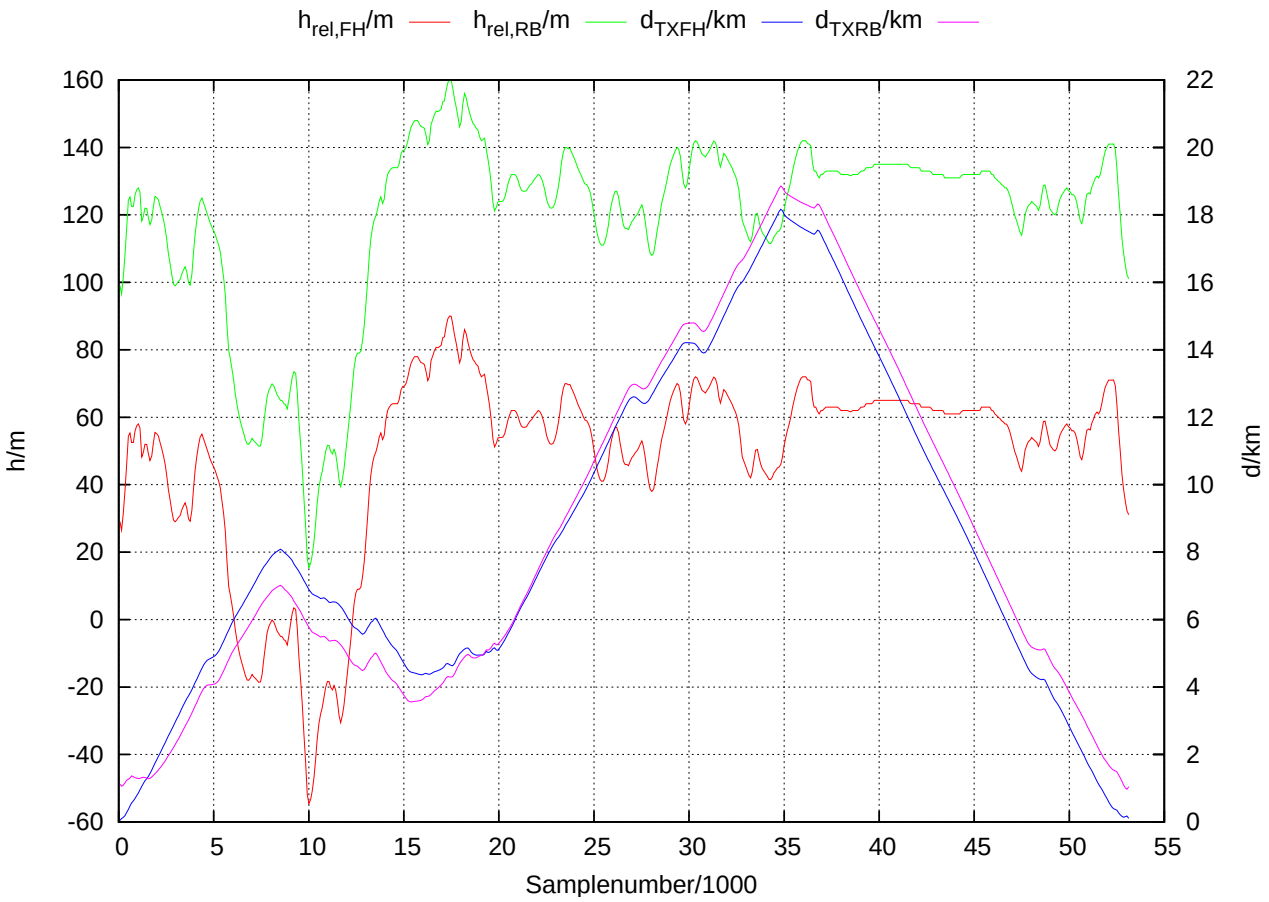

Fig. 3.12: Heights and distances along the route to the individual transmitters

Finally, 3.13 shows the speed profile of a typical measurement run during phase 1 (winter, see the following chapter for details). The values are smoothed using a sliding window of 50 samples.

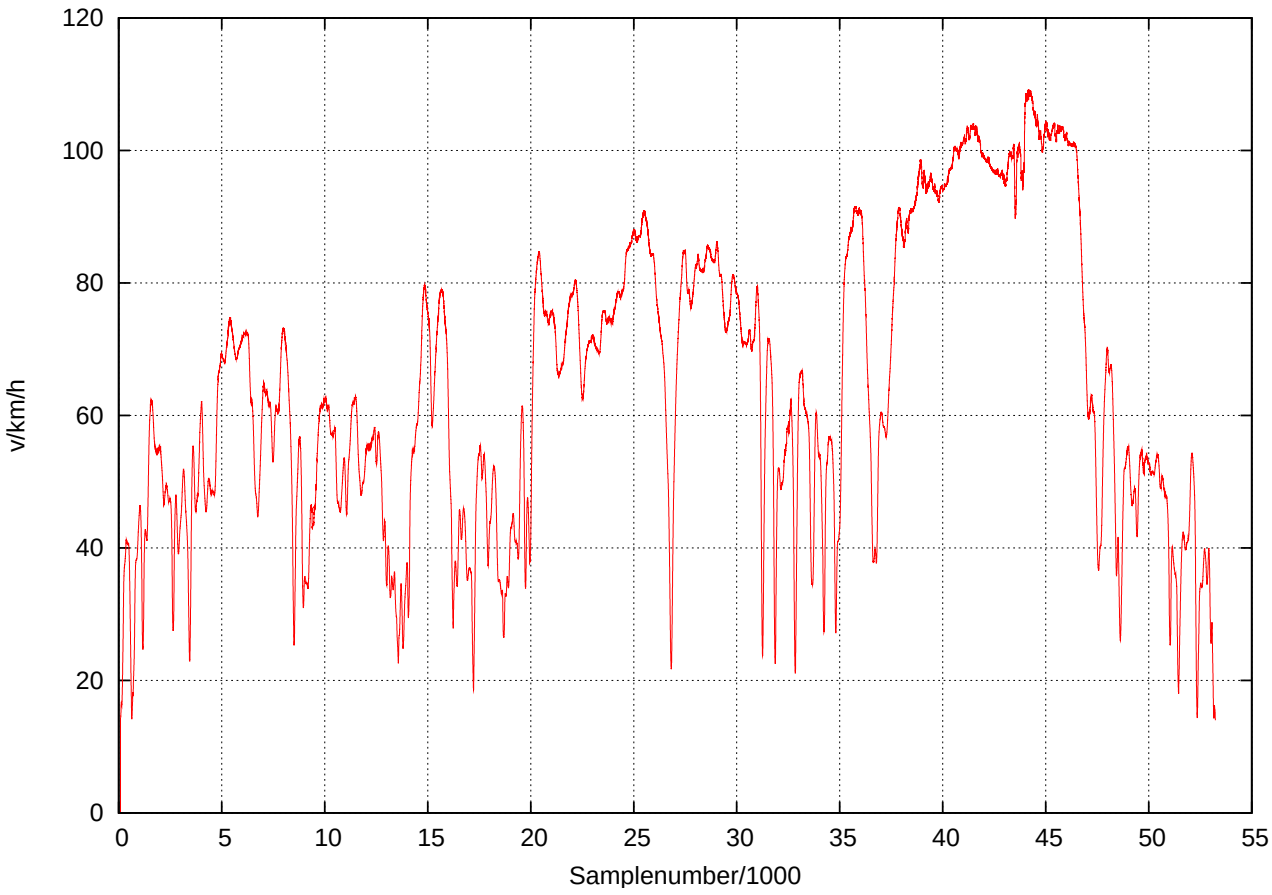

Fig. 3.13: Typical speed profile during a measurement run in phase 1

4 Phase I: adjacent channel interference scenario, fieldstrength distribution

4.1 Phase I key parameters

This first phase of the trial is gouverned by the following issues:

- TX FH is operated on channel 10C with 90 W.
- TX RB is operated on channel 10B, radiating with 135 W in the main lobe.
- weather conditions: snow / ice

4.2 Adjacent channel interference scenario

It became evident very soon that this interference scenario would not lead to interesting results due to the fact that there simply were only a few, selected spots in the Kaiserslautern area where interferences between both could be noted. The differences in radiated power between both transmitters weren't high enough to get serious measurements going. Thus, the operating frequencies had to be changed to a co-channel interference scenario, c.f. the following chapters. Some measurements done in this phase (records of uninterfered transmissions from the individual transmitters) are also valid for the next phase and will be discussed there. Furthermore, the setup was used to get an impression of both transmitter's performance. On this basis, the measurement route for the mobile recordings during this trial was chosen, see also sec. 3.5.

4.3 Fieldstrenghth distribution of both transmitters

The fieldstrength of both individual transmitters in the height of the measurement's van rooftop (about 2 m above ground) is shown in fig.'s 4.1 and 4.2. A conversion to the input power level in dBm at the receiver's input can be achieved by subtracting 118.6 dB from the fieldstrength value. The values in each pixel reflect the median of the samples levels that are contained in the area covered by one pixel. The color scales on both figures are equal. Although the total radiated power by TX RB is higher in the main lobe (135 W) than the power of TX FH (90 W, omnidirectional), TX RB is never touched by the route as close as TX FH. Thus, fieldstrengths from TX RB larger than 81 dBµV/m were neve registered.
Inspecting the distribution of TX FH's fieldstrength, it is easy to see that the transmitter can cover the western area to the motorway much better than the eastern area. The city's region along the route is covered with plenty of fieldstrength, so no reception problems are to be expected. For the northern and far eastern / far western route sections, the low antenna height limits the propagation's path evidently, as the line of sight is obscured by the hillshades that are enclosed by the route.
On the contrary, the antenna pattern of TX RB is easy to reflect by observation of fig. 4.2. Since the antenna has got quite a clear sight onto the route (see also fig.3.11), the hilly areas in the antenna's front lobe can be covered with a quite smooth and ample fieldstrength.

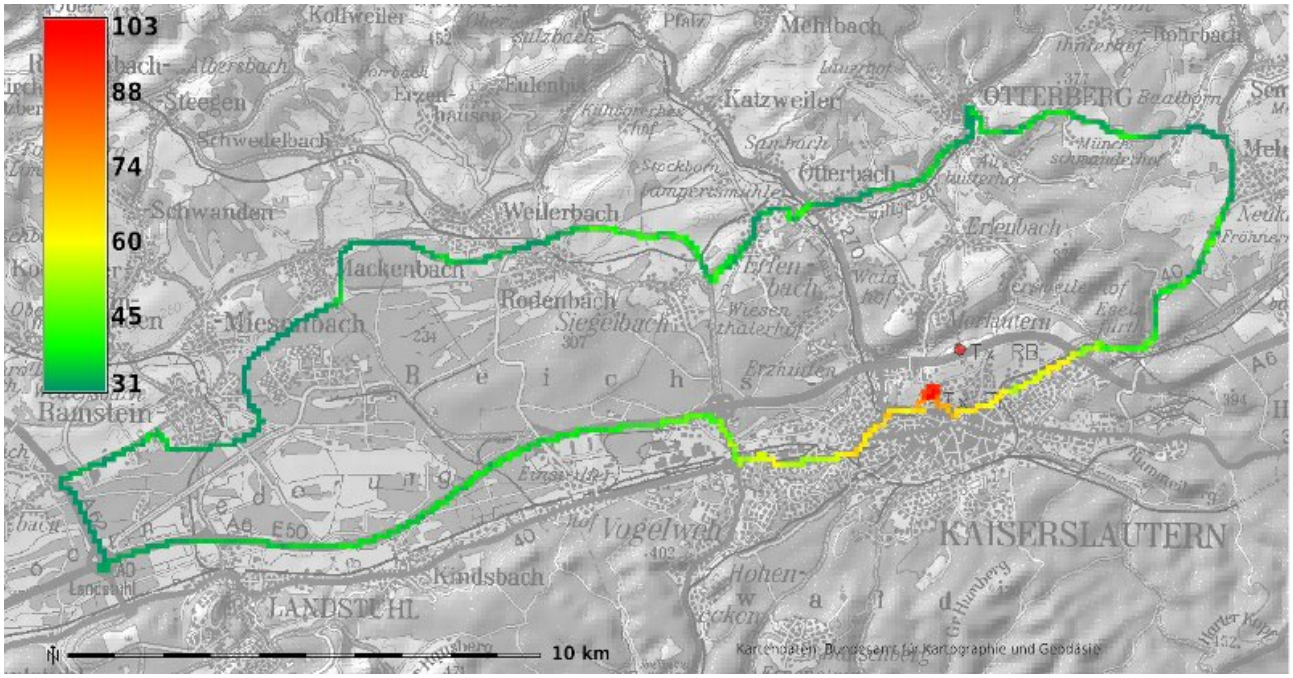

Fig. 4.1: Fieldstrength of TX FH along the route

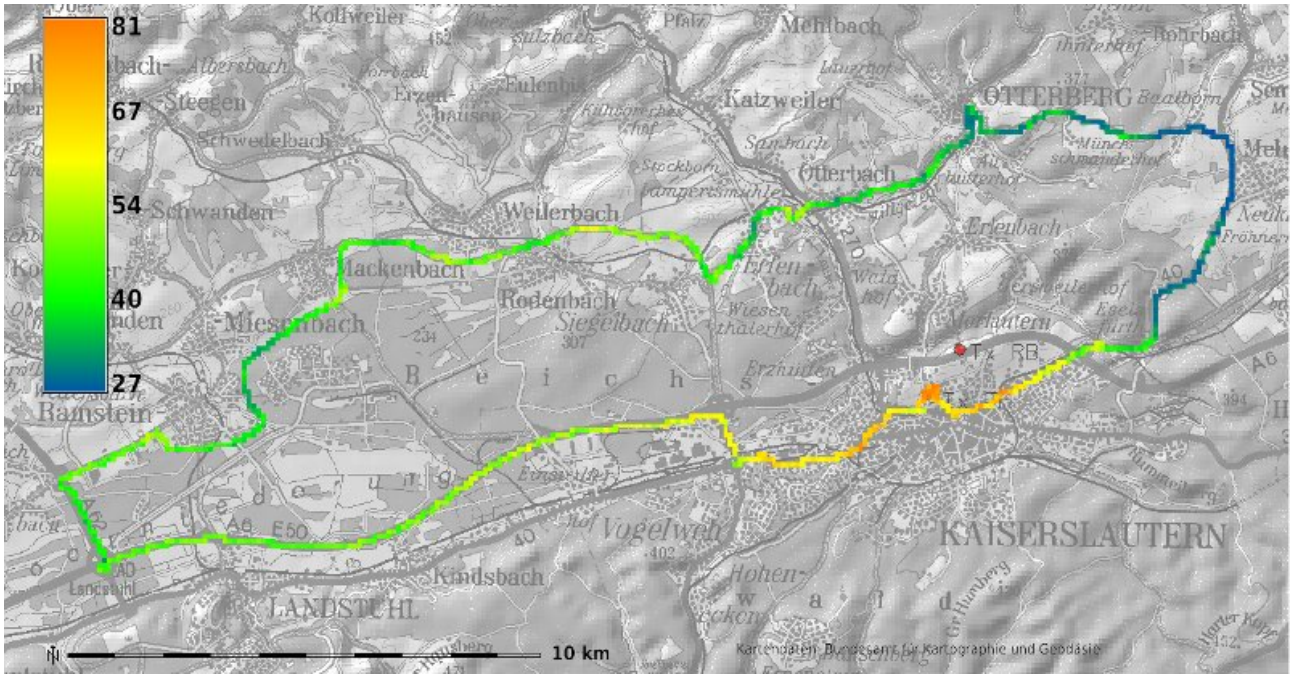

Fig. 4.2: Fieldstrength of TX RB along the route

Figure 4.3 shows the DRM$^+$-performance along the route. A comparison with the fieldstrength plot reveals that a bad decoding state usually occurs in those regions where the fieldstrengths are in the lowest (dark green) category.

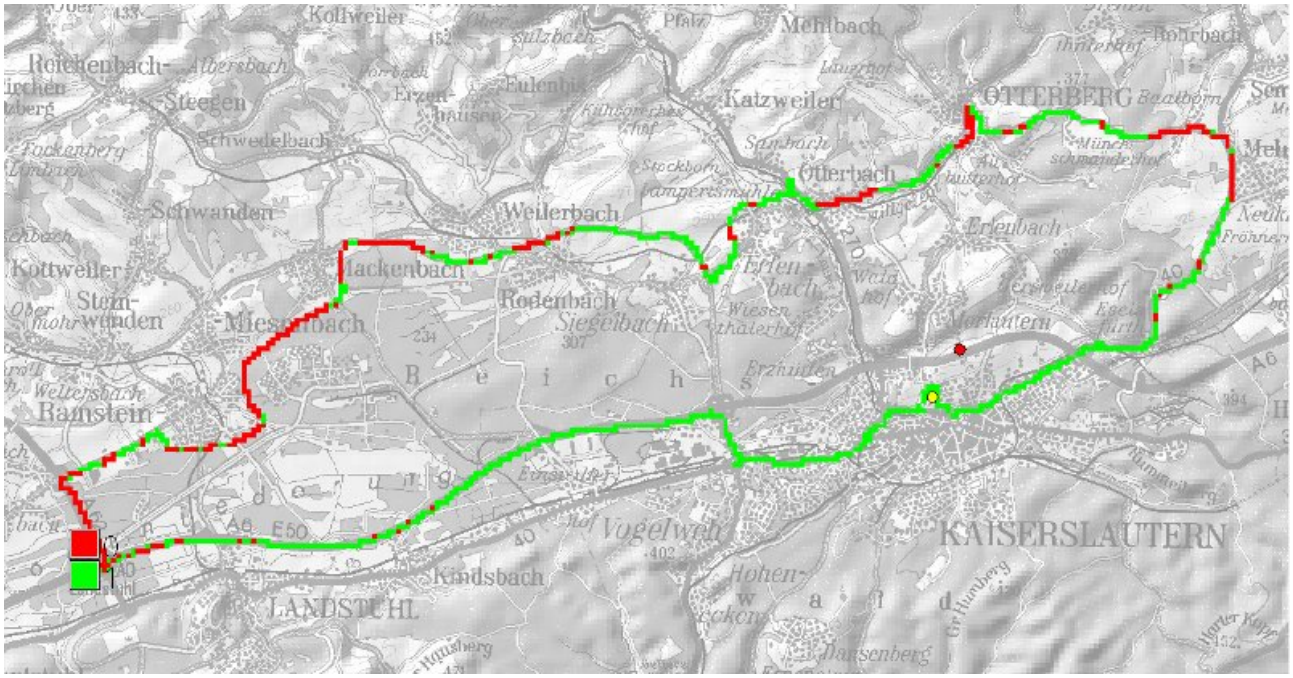

Fig. 4.3: DRM^{+} (16-QAM) reception quality along the route, no interference from TX RB

5 Phase II: Co-channel interference scenario

5.1 Phase II key parameters

The trial's second phase is gouverned by the following issues:

- TX FH can be operated on channel 10B
- TX RB can be operated on channel 10B
- TX RB's power is 135 W in the main lobe, see also section 5.3
- TX FH's maximum EIRP is limited to W 90.
- weather conditions: early spring

5.2 DRM$^+$

To check the route's choice in terms of 'hitting the coverage border', two simple test drives were made with TX RB switched off. The test was just to drive far enough too see that reception break down completely. The results are shown in figures 5.1 resp. fig. 5.2. The raw, instantenous Bit-error-rate is shown instead of the ususal raster-based approach since both figures are meant to be an overview. One has to remember that the total achievable coverage in both modes (DRM$^+$ / DAB) is a bit higher, due to the antenna coupler's losses of 3 dB (the reception antenna's path is split in two – one path for the receiver, one path for the fieldstrength measurement). This restriction always applies to all mobile measurement scenarios shown throughout the report, such that all measurement result keep comparable.

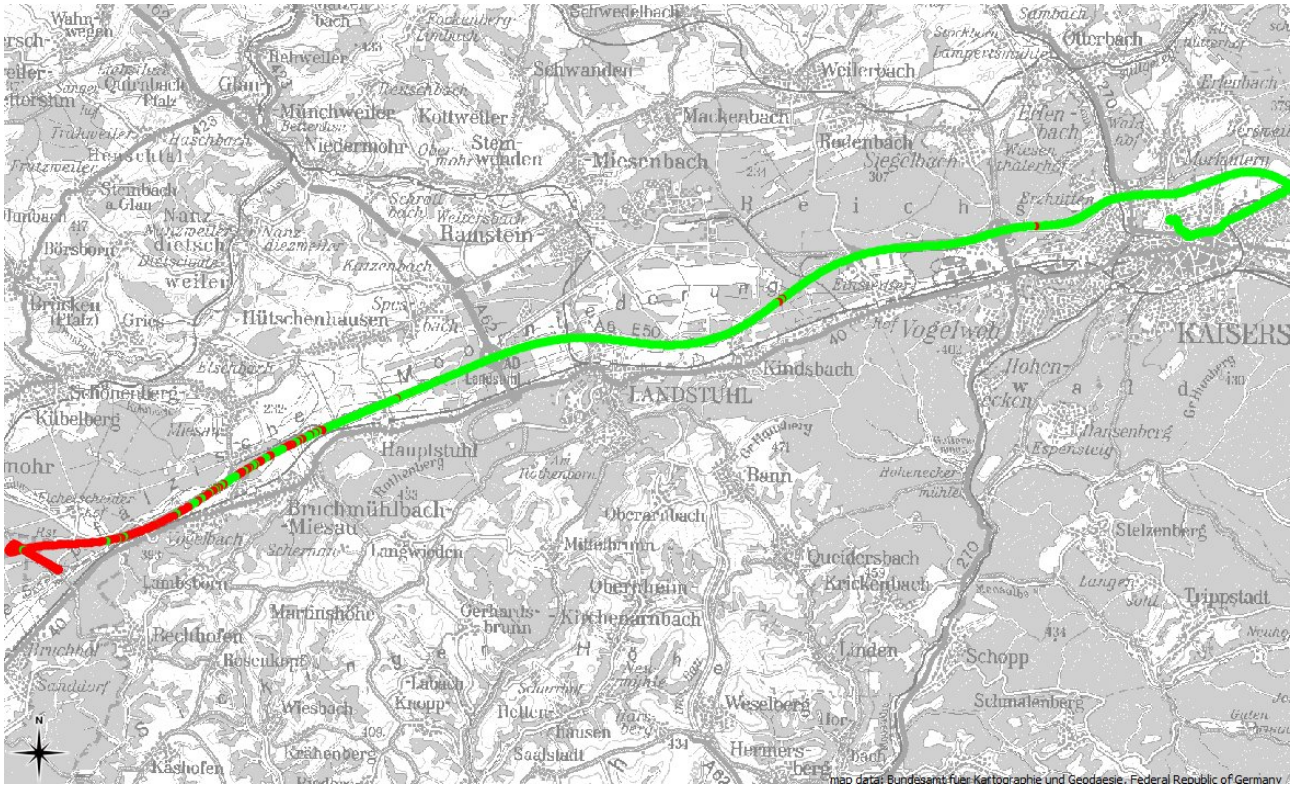

Fig. 5.1: Coverage test drive, 4-QAM-mode

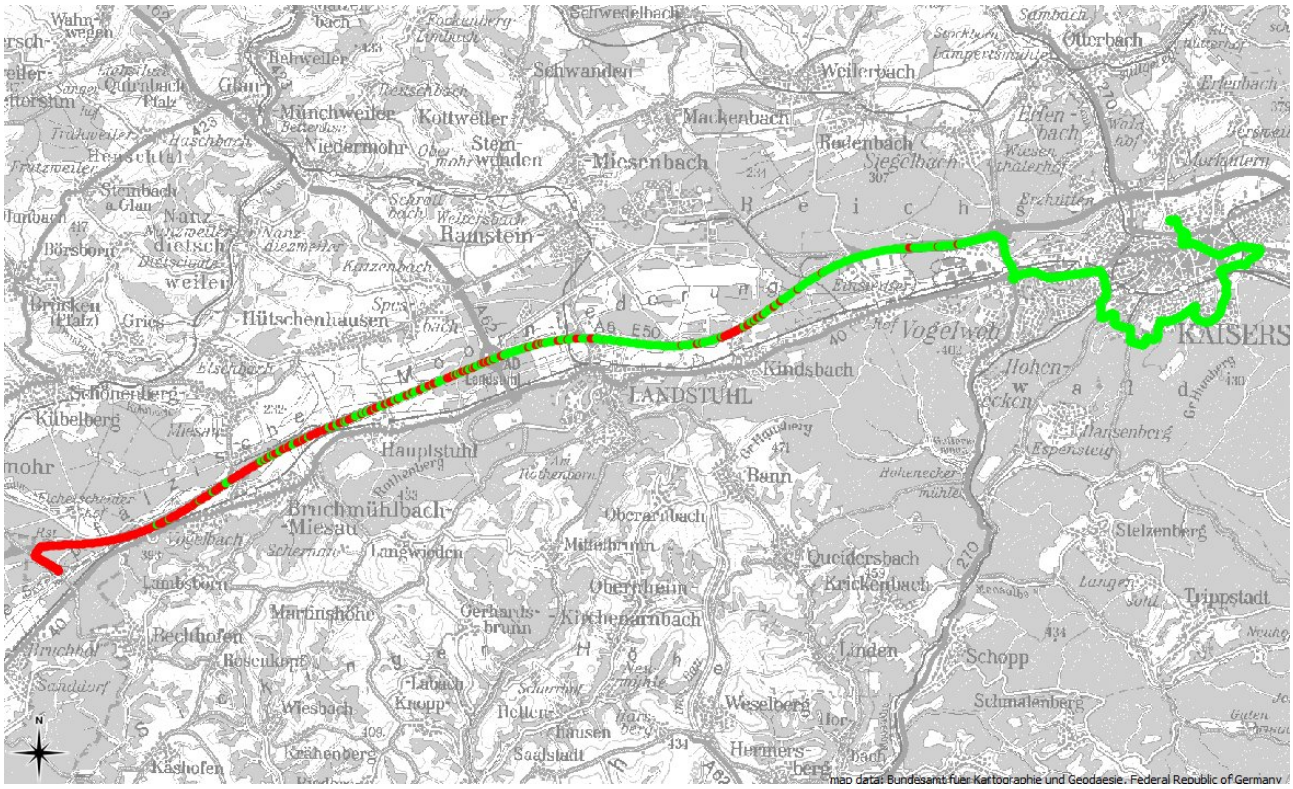

Fig. 5.2: Coverage test drive, 16-QAM-mode

Several test runs were made to record the interference situation regarding DAB interference into DRM$^+$. They are shown in the 3rd phase, since they were repeated during that time. A comparison has shown that no noteable difference in the general result from that measurements exist, so there's

no need at this chapter to bascially show the same things again.

5.3 DAB and DAB$^+$

Some test runs on the performance of the DAB and DAB$^+$-reception were done during this phase. The laboratoy measurements suggest that a protection ratio of about 10 dB is needed. Comparing fig. 4.1 and fig. 4.2 hints that there are many zones where the fieldstrength of both transmitters are not in this range. Thus, the power of the DAB-transmitter was raised to 270 W, to ensure that as many areas as possible can fulfil the protection ratio.

Fig. 5.3 show the differences of the fieldstrength's along the route. It can be seen the difference is usually in the 10 dB range, when the fiedlstrength of TX RB is taken as reference. Thus, positive values represent areas where TX RB is stronger than TX FH and vice versa. One has to remember that the fieldstrength in the routes eastern and northern parts is generally low from both transmitters. This means, that the best approximations to verify the protection ratio is in the regions closer to the transmitters, where sufficent measurement dynamics are availabe.

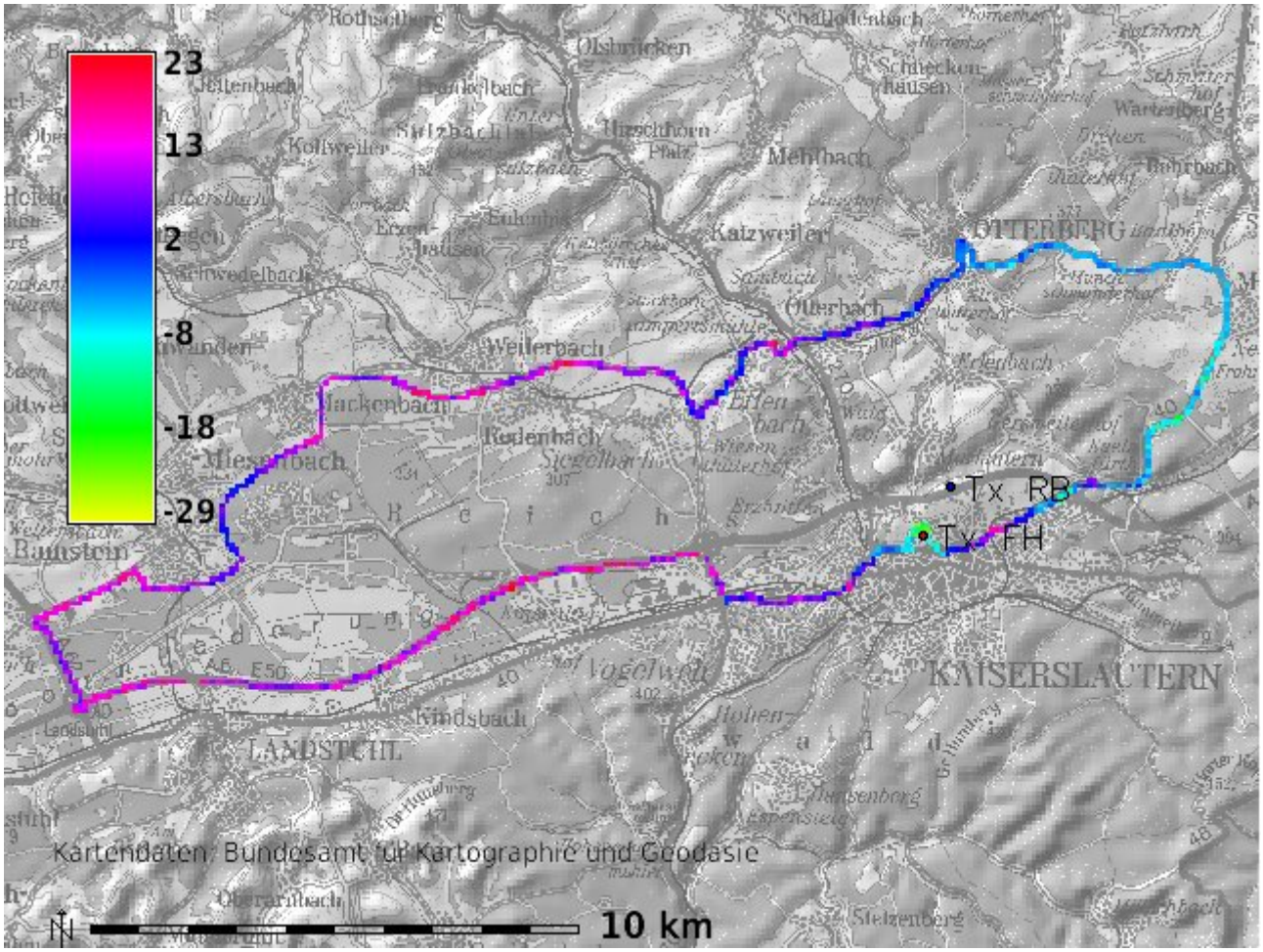

Fig. 5.3: Difference of TX RB's and TX FH's fieldstrength along the route

The first measurement run shows the DAB-coverage when TX FH is switched off, cf. fig. 5.4. Coverage is given along the whole route except in TX RB's rear lobe and some gaps in the route's north-west.

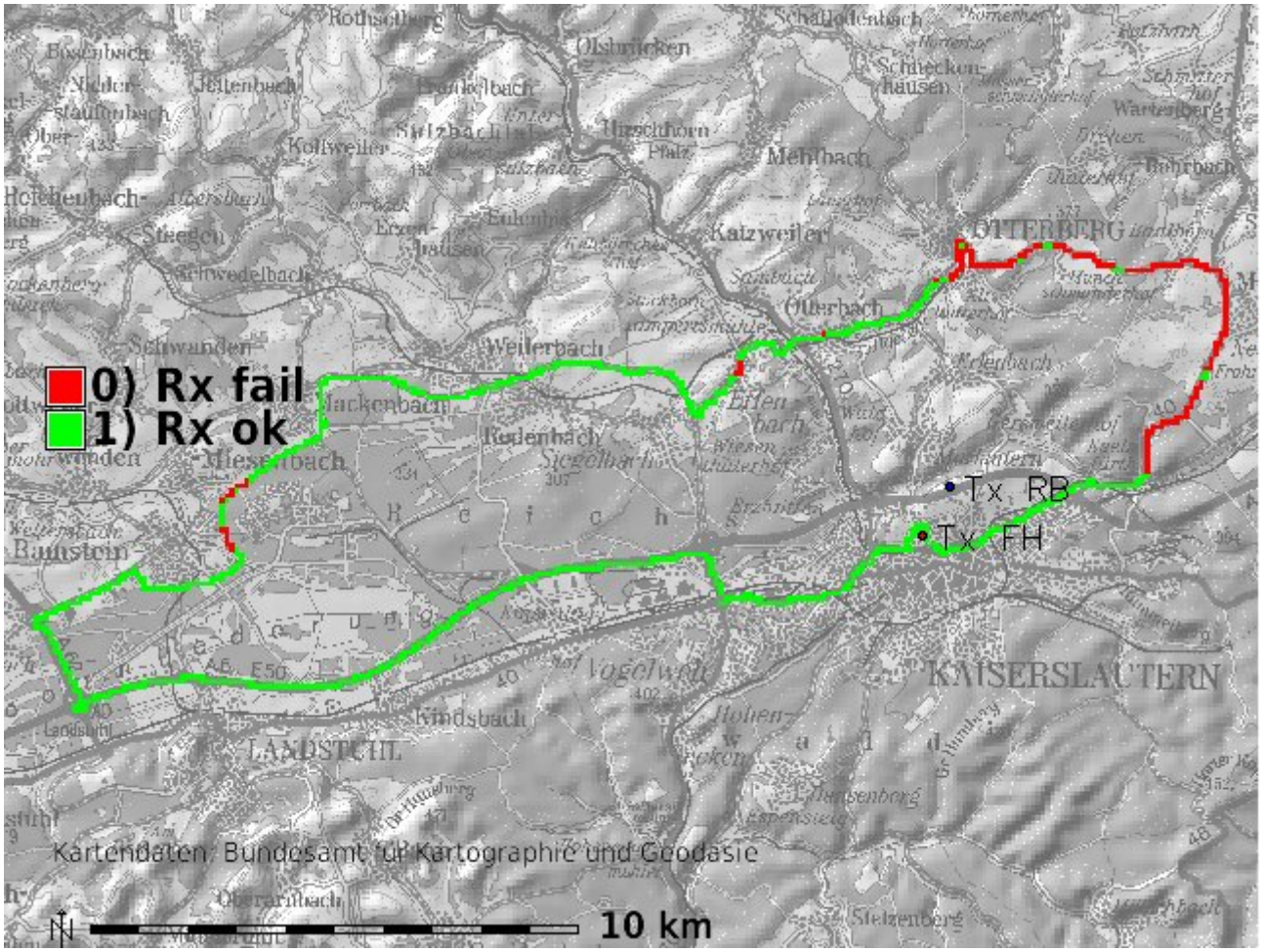

Fig. 5.4: DAB coverage from TX RB while TX FH is switched off

The following fig. 5.5 shows the coverage situation when TX FH is switched on. A comparison with the figure beforehand shows no significant differences, except the area close to TX FH and an earlier dropout in the eastern area. A further look onto fig. 5.3 shows that these regions have a difference in fieldstrength in the range of $-8.. -10\,\mathrm{dB}$ and beyond (cyan regions and below), which means that the DRM$^+$-fieldstrength is higher by that amount. This roughly matches the laboratory value of 10 dB.

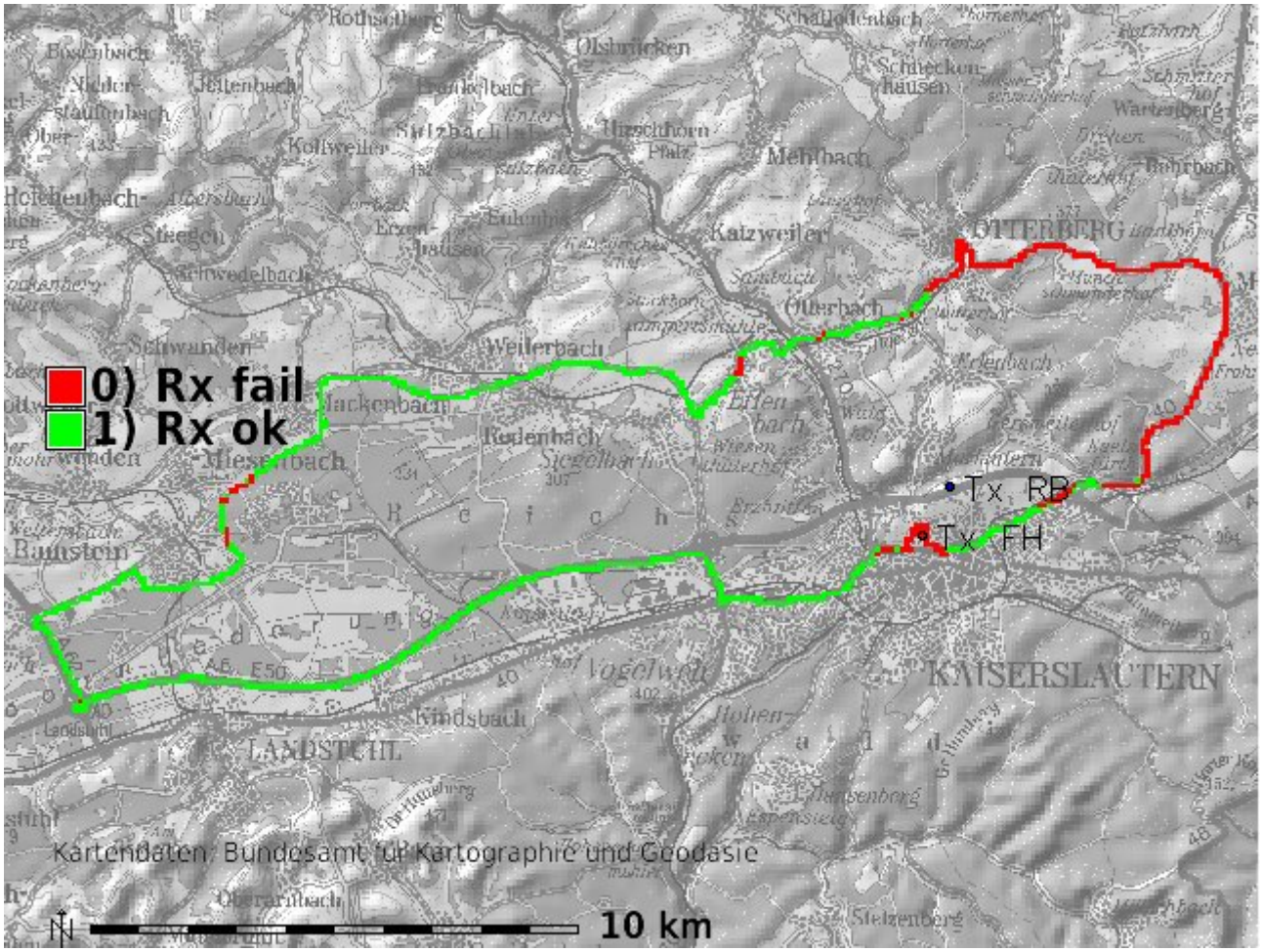

Fig. 5.5: DAB coverage from TX RB while TX FH switched on

The next figure (fig. 5.6 shows the result of a measurement run where two DRM$^+$-multiplexes are radiated by TX FH. The total available power of W90 is distributed equally to both blocks. Each block is shifted by 100 kHz up / down from block 10B's center frequency and thus are spearated 200 kHz apart. Thus, the situation can be compared to the situations with two active DRM$^+$-multiplexes in [Köh09, sec. 5.3.4]. These laboratory results show only a difference of 1 dB in the protection ratio. The measurement run's result in fig. 5.6 shows only minor differences compared to the situation where only one DRM$^+$-multiplex was radiated. This result tends to harden the correctness of the laboratory measurements.

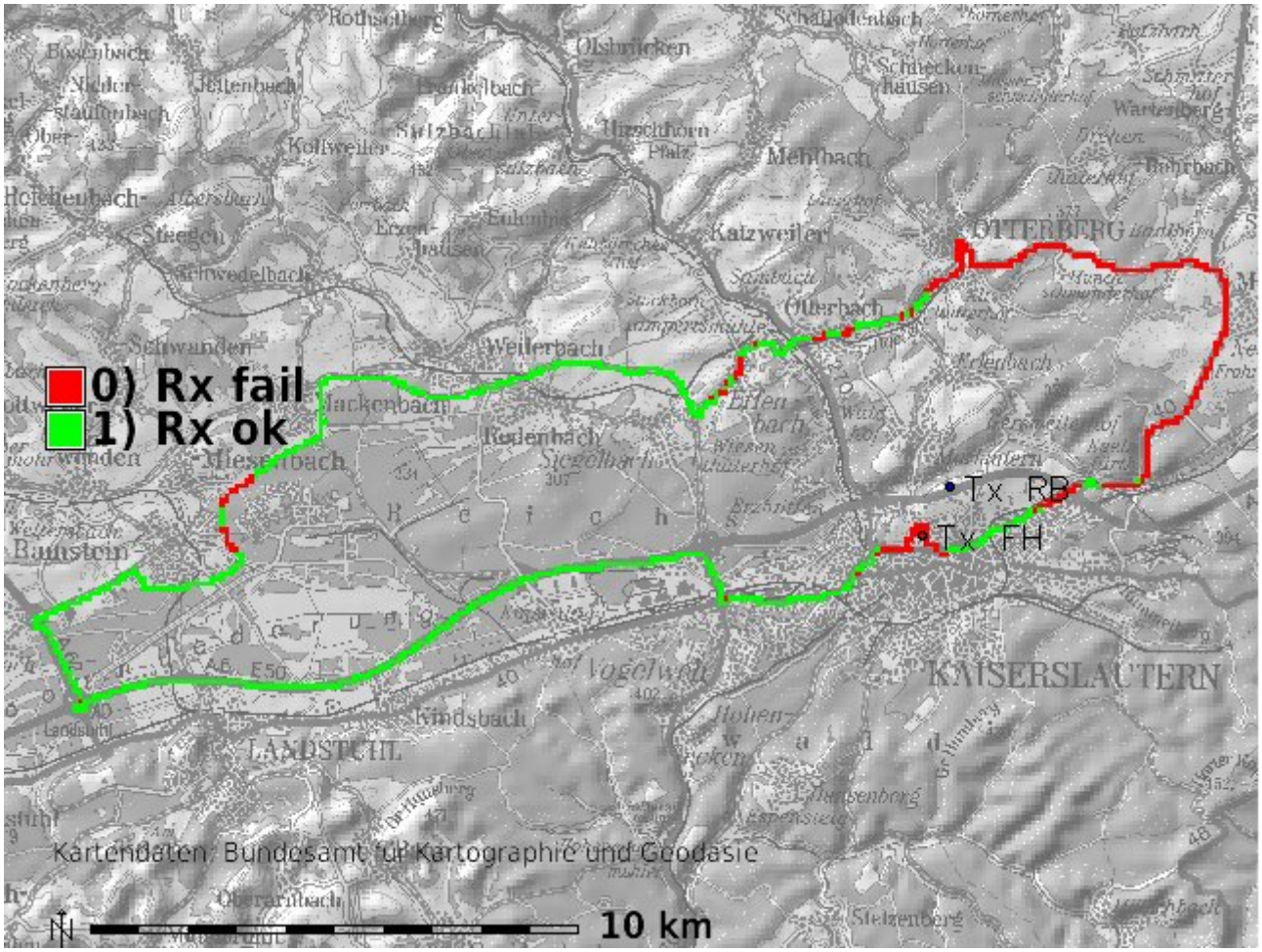

Fig. 5.6: DAB coverage from TX RB while TX FH emits two multiplexes

Furthermore, the DAB-transmitter was switched into DAB$^+$-mode. The output power, center frequency and content was kept constant. Since no measurement receiver was available for this coding scheme, a subjective comparison between the robustness of both systems was made. For this a consumer receiver capable of DAB and DAB$^+$-decoding was mounted into the measurement van and two measurement runs in direct sucession were done. On a subjective scale, the listening experience on the coverage border is basically the same for both coding schemes. Nontheless, the (DAB$^+$'s) audio decoders rapid muting property is more satisfying than the gargling and hissing sound by DAB's Musicam-Codec on the coverage border. Sadly, the points of failure don't shift significantly due to the system's change. To give an example, the passage of Erfenbach was always dominated by audio hisses in DAB-mode. The switchover to DAB$^+$led to no change at all; the fading gaps were too deep and still to long to be compensated by the transmission chain – the DAB$^+$-decoder started to flutter at the same spots (like the start of a road-crossing) as before the switchover. To express more general: the differences in the enviroment of the measurement route is extremly small.

6 Phase III: Co-channel interfernce scenario, higher power on TX FH

6.1 Phase III key parameters

The trial's third phase is gouverned by the following issues:

- TX FH and TX RB can both operated on channel 10B
- TX RB's power is 135 W in the main lobe
- TX FH's maximum EIRP is boosted to 180 W.
- weather conditions: summer

6.2 Fieldstrength considerations

Prior to anything else, the differences in fieldstrength excited by both transmitters is shown in figure 6.1. The route can roughly be separated into three sections: one section where the level of TX FH is dominant (i.e. in TX RB's backlobe and right in the vicinity of TX FH); one section where both levels are roughly equal (on various occasions, cyan color) and one section, where TX RB is usually the stronger one (green areas). The radiated powers used for this measurement run are as noted above on the start of this chapter.

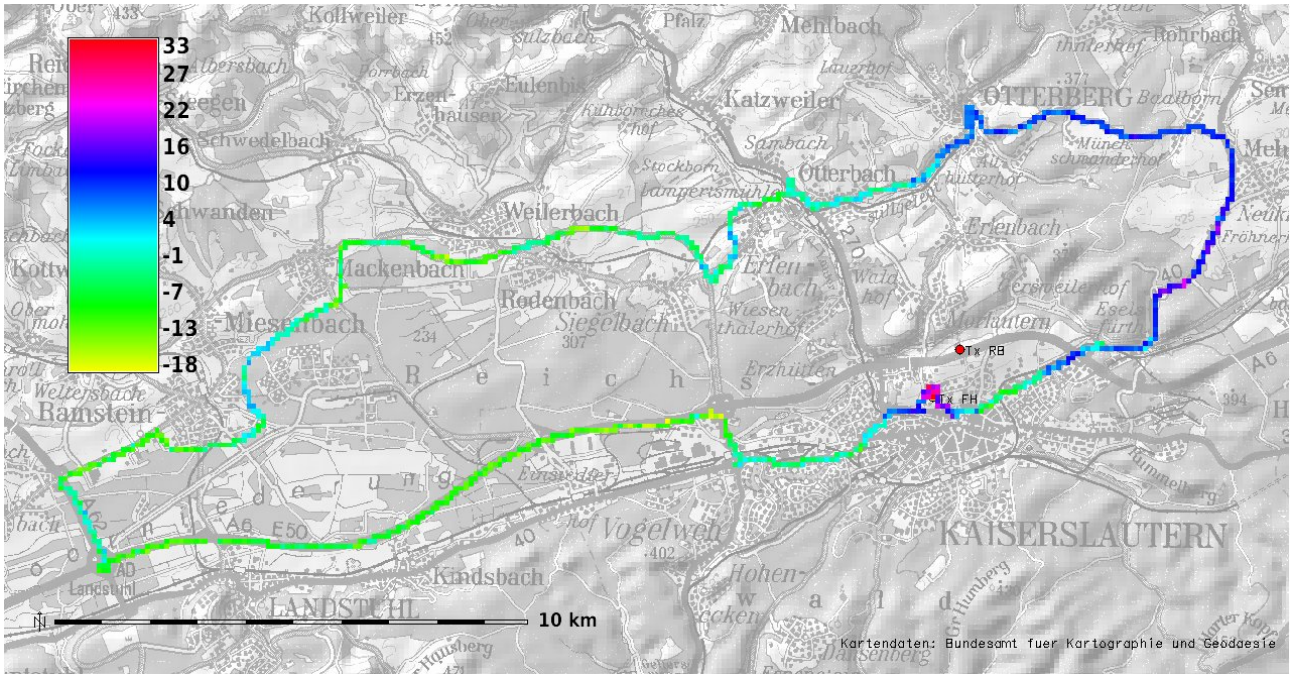

Fig. 6.1: Difference of fieldstrengths by both transmitters: $E_{FH} - E_{RB}$

6.3 Interference tests vs. DAB for the DRM$^+$ with 16-QAM-MSC-modulation and comparison with planning predictions

First, the coverage achieved in 4-QAM-Mode is shown in fig. 6.2. Reception is good along almost the whole route.

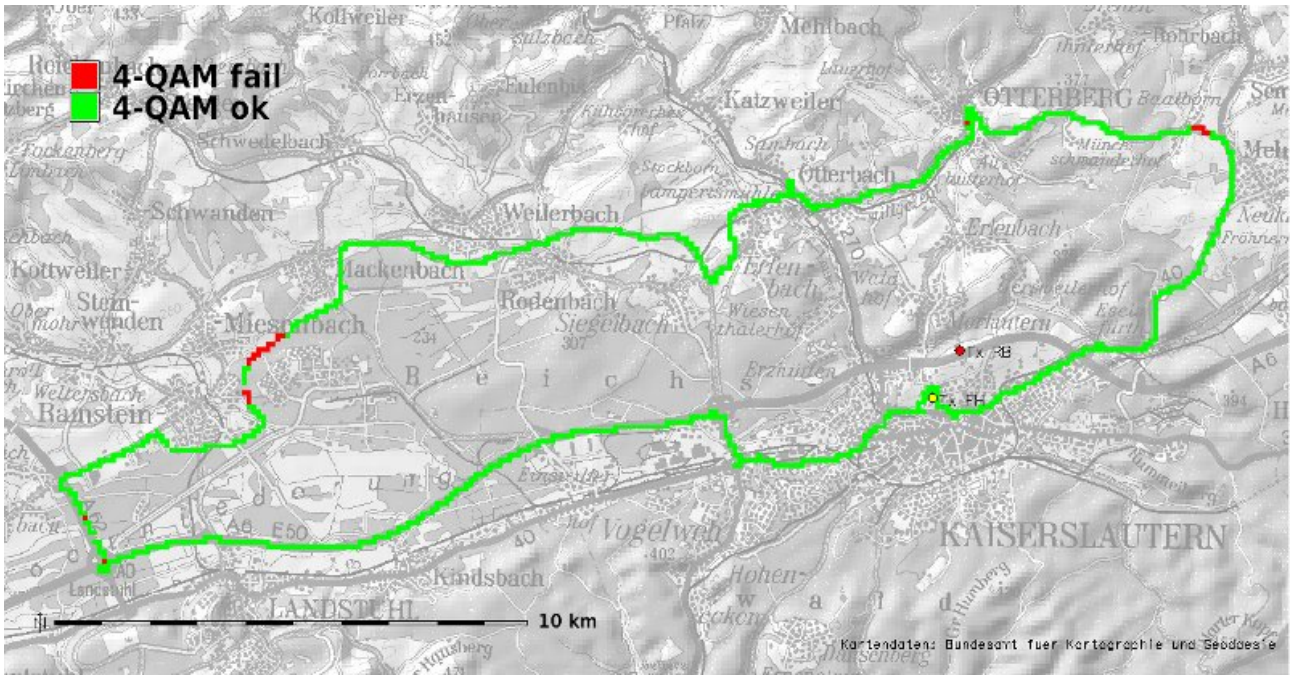

Fig. 6.2: DRM$^+$-coverage with 180 W, 4-QAM

Next, TX RB is turned on an the previous measurement is repeated. The result is shown in fig. 6.3. Combining this with fig. 6.1, one can note that reception is only possible in those areas where at least the cyan color shows up which means that both transmitters raise roughly the same fieldstrength at these regions.

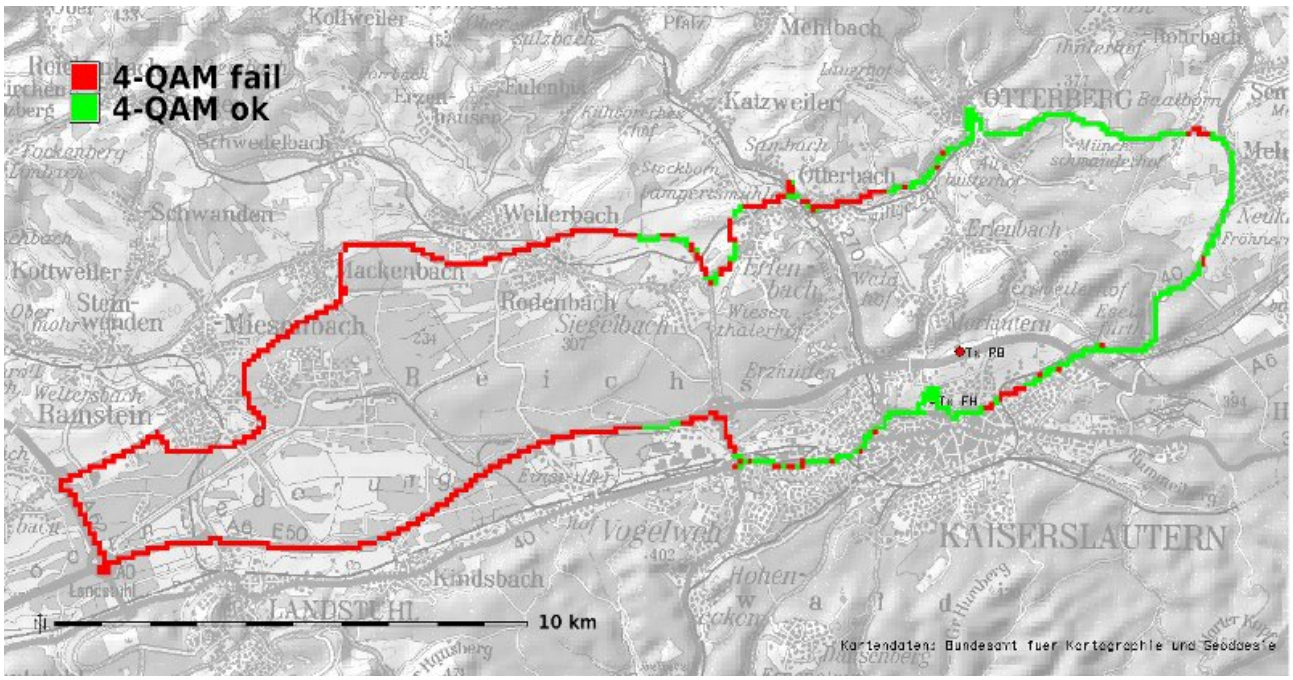

Fig. 6.3: DRM$^+$-coverage with 180 W, 4-QAM, co-channel interference

Figure 6.4 shows an exemplary planning of TX FH's coverage using the data obtained from laboratory measurements under the assumption, that the transmitter's output-power is 180 W, TX RB is turned off, that the MSC-modulation is 4-QAM and a $\lambda/4$-dipole in approx. 2 m above ground is used for reception. The planning raster is 100 m × 100 m, as for the meaured data. The planning relies on fieldstrength values with a location probability of 95%, categorizing

- yellow areas: reception is bad / not possible. Fieldstrength is up to 44 dBµV/m
- green areas: reception might fail. Fieldstrength is between 44 dBµV/m and 58 dBµV/m.
- blue areas: reception is possible. The fieldstrength is 58 dBµV/m and beyond.

The planning results are shown is shaded colors, while the measured data are shown with solid colors. Red rasters indicate that reception has failed, while dark blue boxes mark the raster pixels where the reception is quasi-error-free.
Comparing both layers indicates that the spots where reception actually fails fall right into the yellow areas and borders of the green areas. Receptions has measured to be robust in the interior sections of the green areas, thus the planning seems to be too pessimistic by a few dB.

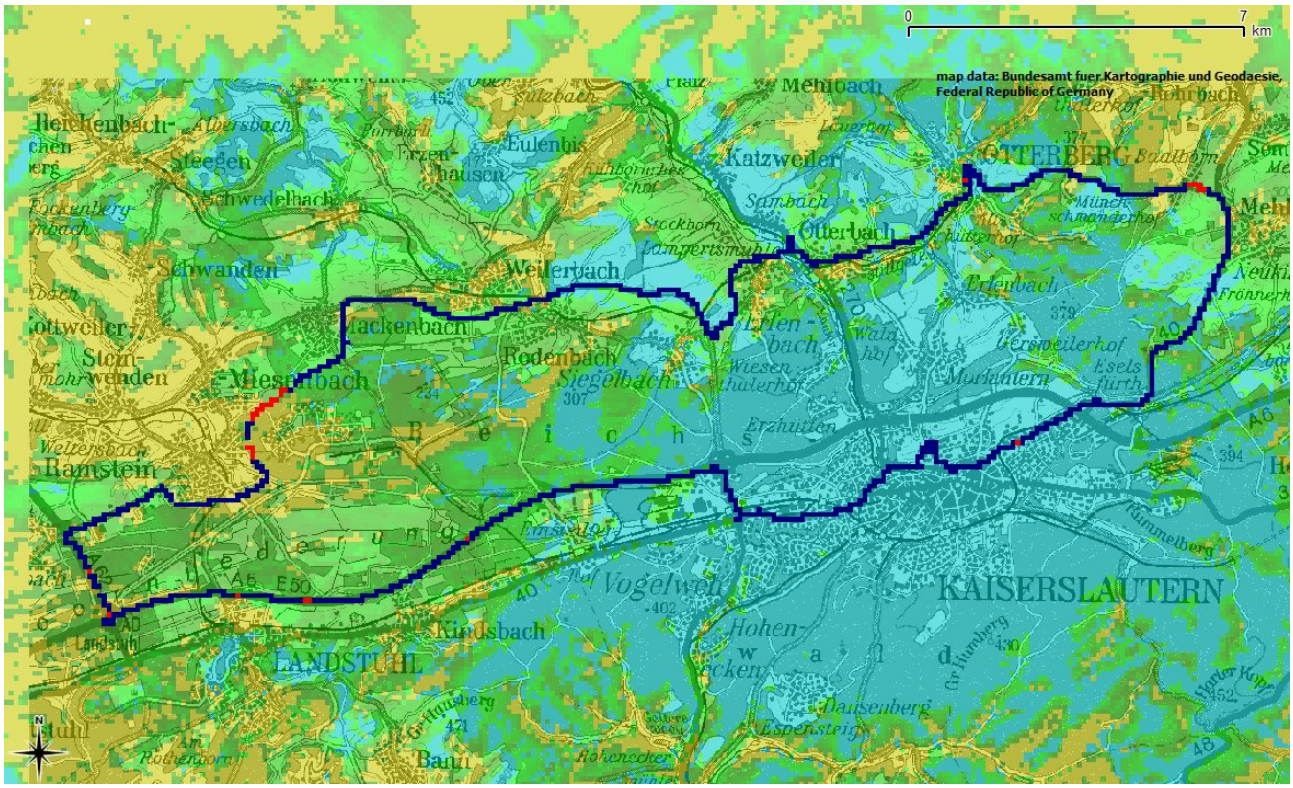

Fig. 6.4: Predicted and measured coverage in 4-QAM-mode: comparison

6.4 Interference tests vs. DAB for DRM$^+$ with 16-QAM MSC-modulation

The figures 6.5 and 6.6 represent the result of the same test, with 16-QAM as the MSC-modulation. A brief look on fig. 6.1 reveals that the areas where reception is possible is shifted to the fieldstrength-rating that fall at least into the blue regions, which means that TX FH is roughly 10 dB stronger than TX RBwith the effect, that the protection ratio is met.
For both cases, it shall be noted that the carrier-to-interference-ratio seen here is influenced by the mobile radio path's, the receiver's intrinsic noise and external interferers like engine noise, sparks from electrical devices, residual fieldstrength from other DAB-services on the co-channel etc. These are the

main reasons why the carrier-to-interference-ratio generally seems to be more demanding as compared to the laboratory measurements in [Köh10].

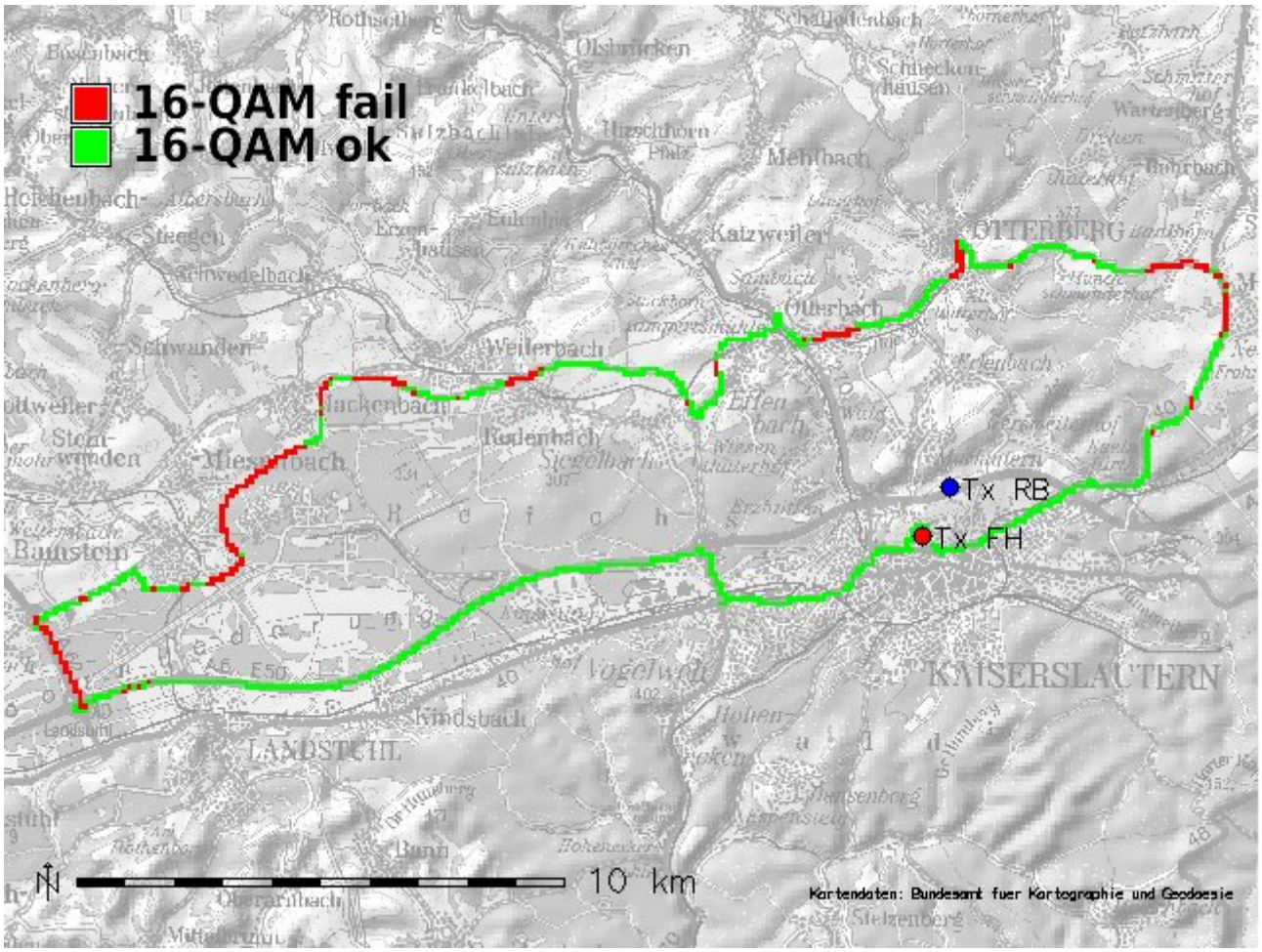

Fig. 6.5: DRM$^+$-coverage with 180 W, 16-QAM

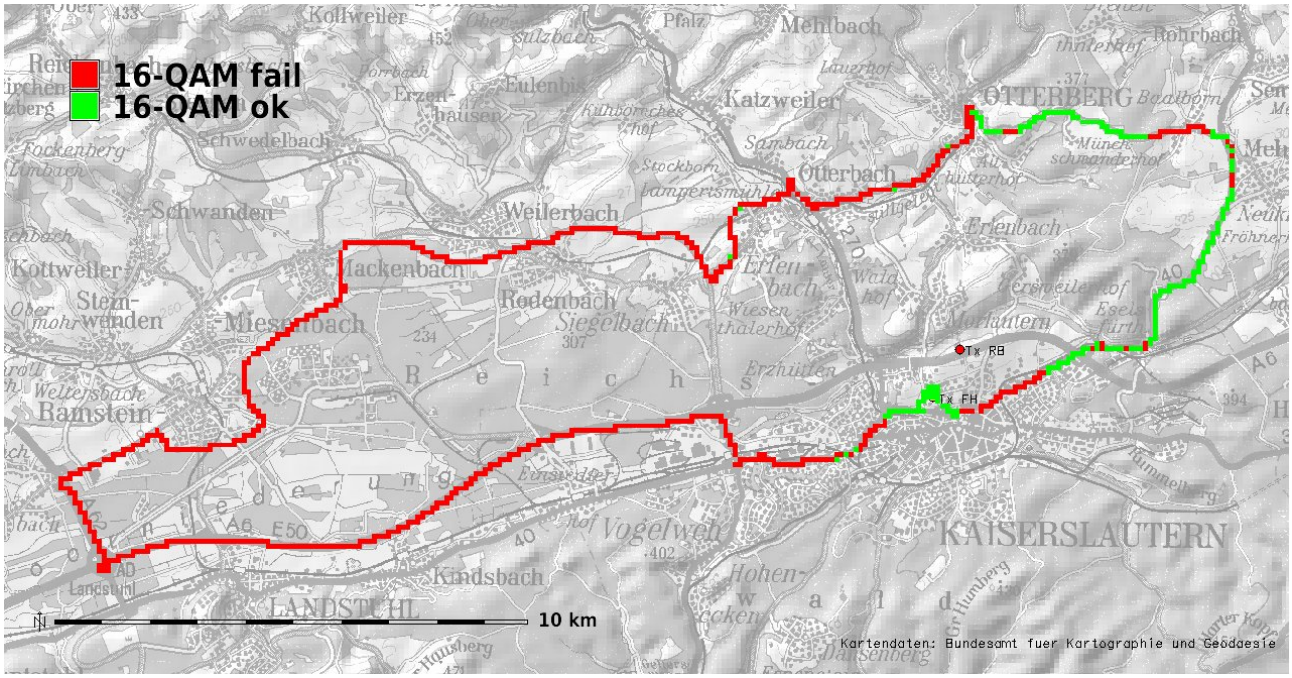

Fig. 6.6: DRM^{+}-coverage with 180 W, 16-QAM, co-channel-interference

7 Stationary measurements

A minor aspect of the trial was the assessment of the stationary protection required for the DRM$^+$ transmitter. For this, thanks to the generous support of the federal network agency of germany, the measurement van known from [SS08] was used. It's main feature is the directional measurement antenna FT01 (c.f. [SS08]), the turnable extendable antenna mast with a max. height of 10 m above ground level and an ample working space along with an long lasting power supply.
The spots indicated in fig. 7.1 were used as measurement locations. Most of them were located along the route, but usually inside of the towns, instead of the roadside. The measurements took place during the first phase and investigate the case of an interference in the co-channel, i.e. DAB and DRM$^+$are operated on exactly the same center frequency.

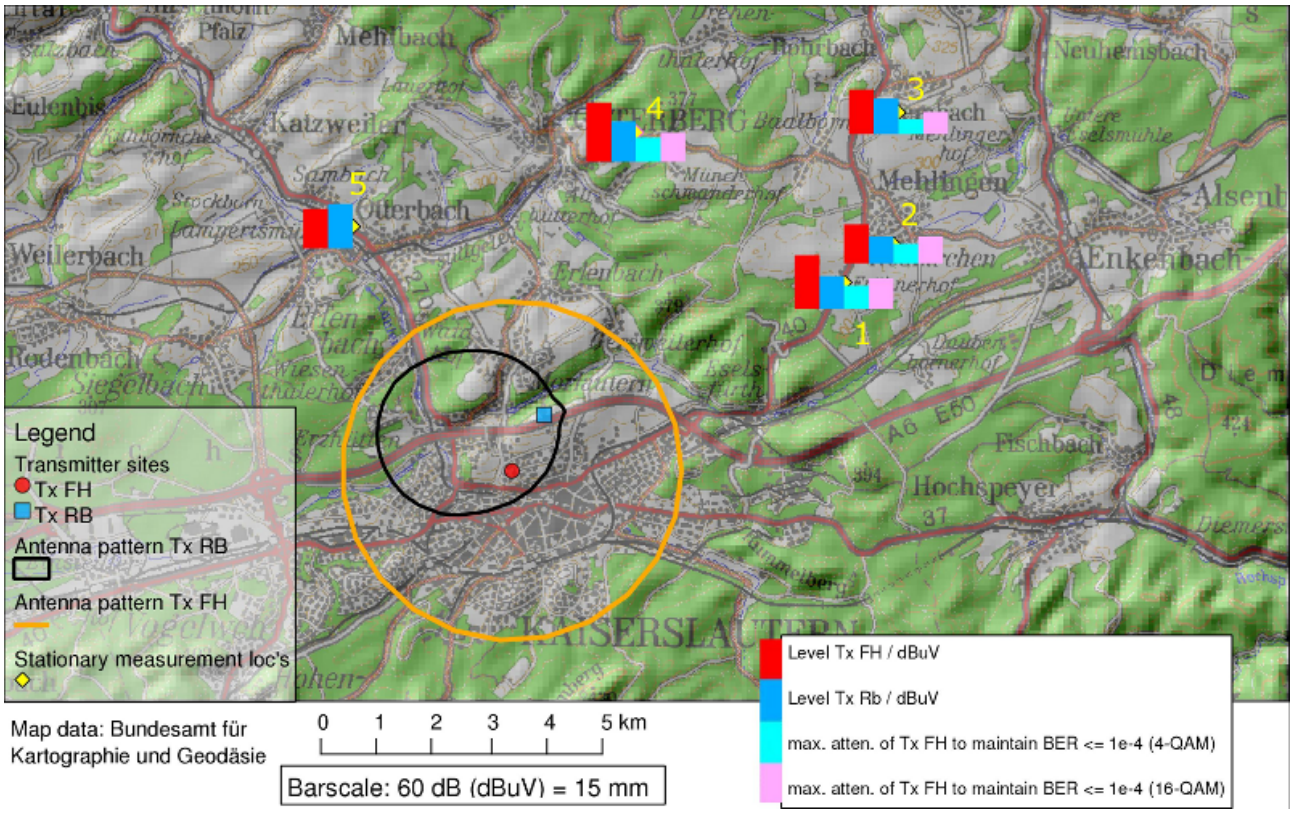

Fig. 7.1: Overview map of the locations and receiver input voltages for stationary measurements

The measurements were conducted as follows: the reception antenna was polarized accordingly to TX FH's polarization, extended up to it's full height and rotated into TX FH's direction. The channel powers of TX FH and TX RB were measured using a spectrum analyzer. Afterwards, the standard receiver for DRM$^+$ was connected. Upon sucessful reception (i.e. BER $\leq 1 \cdot 10^{-4}$), TX FH's transmit power was reduced by using the remote access to TX FH's controls, until the BER reached it's limit. The measurement locations are shown in fig. 7.1. Furthermore, the receiver input levels and the attenuation values for the 4- resp. the 16-QAM-MSC modulation on the DRM$^+$-signal are shown. Additionaly, the assorted numbers are tabulated in tab. 7.1 and evaulated in tab. 7.2. On the tables, the columns are titled as follows: the measurement point's number is listed in column 'MP-Nr.', a

descriptive name is given in column 'MP-Name'. The channel powers (expressed as voltage levels in dBµV) of the wanted transmitter (TX FH) and the unwanted transmitter (TX RB) are given in the columns 'U(TX FH)' resp. U(TX RB)'. The additional attenuation of TX FH is noted in the columns 'Atten(TX FH),{16|4}-QAM'. The difference in channel powers (including the extra attenuation at TX FH) makes up the 'field protection ratio', as noted in tab. 7.2, columns 'C/I {16|4}-QAM'. The values from the laboratory measurements as found in [Köh10, chap. 5] are noted in this table as reference values. Finally, the columns '$\Delta_{C/I}$' show the difference of the C/I-values from the laboratory and the field measurements. The value of 0 dBr means that no difference for the required protection has been found. A value less than 0 dBr means that less protection was needed than observed in the lab; a value above 0 dBr means, that more protection than in the lab was needed. A '%'-sign indicates that the receiver voltage wasn't high enough to decode the MSC, thus nothing more can be stated about the situation on that measurement location.

MP-Nr.	MP-Name	U(TX FH)	U(TX RB)	Atten(TX FH),16-QAM	Atten(TX FH),4-QAM
1	Frönerhof	44 dBµV	27 dBµV	19 dB	25 dB
2	Mehlingen	38 dBµV	23 dBµV	17 dB	23 dB
3	Sembach Airbase	42 dBµV	30 dBµV	13 dB	19 dB
4	Otterbach	33 dBµV	38 dBµV	%	0 dB
5	L382	55 dBµV	35 dBµV	21 dB	25 dB

Tab. 7.1: Stationary measurement values

MP-Nr.	MP-Name	C/I 16-QAM	C/I 4-QAM	$\Delta_{C/I}$ (16-QAM)	$\Delta_{C/I}$ (4-QAM)
1	Frönerhof	−2 dB	−8 dB	−2 dBr	−3 dBr
2	Mehlingen	−2 dB	−8 dB	−2 dBr	−3 dBr
3	Sembach Airbase	−1 dB	−7 dB	−1 dBr	−2 dBr
4	Otterbach	%	−5 dB	%	0 dBr
5	L382	−1 dB	−5 dB	−1 dBr	0 dBr

Tab. 7.2: Stationary measurement evaulation: protection values (field) vs. protection ratios (laboratory). Reference C/I derived in laboratory measurements taken as 0 dBr: 0 dB for 16-QAM; −5 dB for 4-QAM.

Differences can be justified especially due to the following items:

- the channel profile of each individual transmitter, which is only flat in conducted measurements.
- the power flux density at the receiver's input is not as constant over time as it is in conducted measurements
- instead of the unwanted signal, the wanted signal was reduced in it's power due to the simple reason that the transmitter used in TX RB at this time didn't allow to reduce the output power beyond a certain point; vice versa, the max. power of both transmitters was limited. Thus, at the reception qualities limit, the receiver was influenced by the interfering signal's power and it's intrinsic noise floor, which never occured during the conducted measurements. The lower power limit for TX RB is the reason for not making up this test regarding the required protection for the DAB-system.

Especially the fact that the measurements often required to operate the receiver with a very low-level input signal and the circumstance that less time than in the lab was available where stationary reception can be assumed (a shorter averaging interval was applied to keep the signal as stationary as possible for the determination of $\overline{\mathrm{BER}}$ compared to a laboratory situation, so higher deviations of the mean value have to be taken into account) shows up for the 4-QAM-results, since the gradient of $\overline{\mathrm{BER}}$ over $\mathrm{SNR}_{\mathrm{Dec}}$ is extremly steep in the region of the targeted Bit-error-ratio.

Although the results obtained are kind of vague, one shall consider the measurement's intention: it merely served as a simple cross-check if the required protection measured in the lab can roughly be found in the field. In all cases / measurement locations, this question can be answered 'yes!', since no value in the figure above is larger than 0 dB and the deviation for the 16-QAM-case isn't larger than 2 dB. For the 4-QAM-case, the deviation is much larger. This seems to stem from the fact that it is much harder hit the point where $\overline{\mathrm{BER}} \leq 1 \cdot 10^{-4}$ is fulfilled at best in an unstable field enviroment paired with the fact that the slope of $\overline{\mathrm{BER}}$ is huge in this area of values. Since the same method was applied in the determination for the 16-QAM-values and the 4-QAM-values, it can be stated that the laboratory values seem to be quite realistic for the co-channel interference situation.

During the 1st phase, a cross-check was made to see if the measured protection ratios also apply in an adjacent channel situation. Since the measurement van used in the measurements described above wasn't attainable in a short period of time, a simpler measurement was made using the standard $\lambda/4$-dipole on top of the universities measurement vehicle. Due to the low antenna height and the fact that the antenna used is not directed, obtaining a good measurement spot where the conditions are stable enough for the measurement period is quite more crucial. For this, a large parking spot in the town's western industrial area (inside the main lobe of TX RB), where the levels from both transmitters offer enough dynamic range was chosen. On this time, the measurement goal was to assess the rough value for the protection required for DAB. Figure 7.2 shows the situation at the measurement point when both transmitters are operated with full power. Figure 7.3 shows the situation when TX FH is operated on the lowest possible channel possible in Block 10C (10C 7^-, in terms of [Köh10]). In the 2nd figure, TX FH was attenuated by 27 dB to obtain stable DAB reception with Rx 3. As it can be seen by the ACPR-values in the figures, the total power difference between both signals is 39 dB (the DAB-signal is 39 dB stronger than the DRM$^+$-signal). The spectrum plots show that the channel profile hasn't changed significantly during the measurement. In the laboratory situation, the required power difference was measured to be 43 dB in a quiet listening enviroment under stable conditions. Thus, the laboratory values are kind of well approximated and in no case the required protection values for the DAB-system are never set too low, considering the values derived in [Köh10].

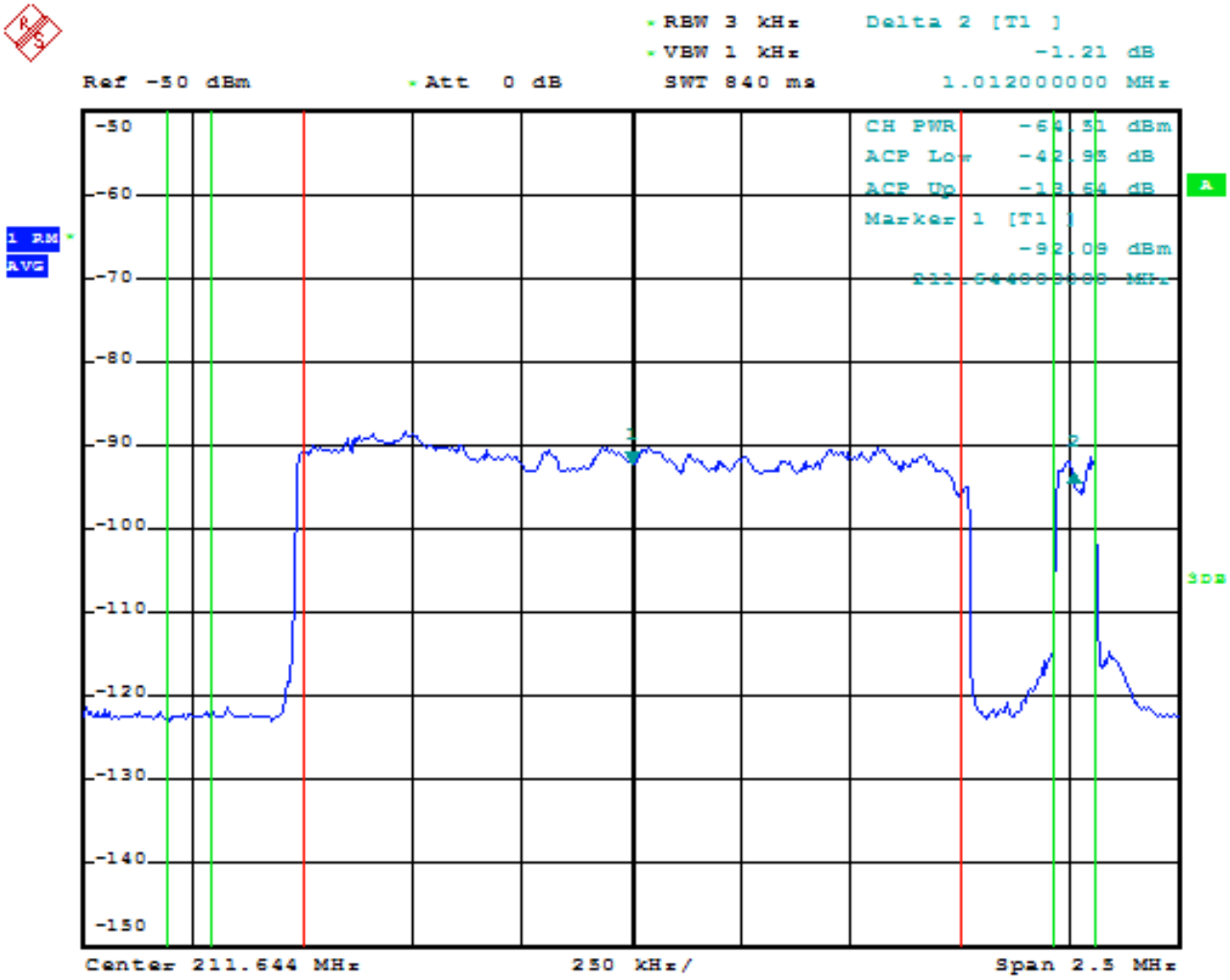

Fig. 7.2: Reference levels for a stationary test measurement

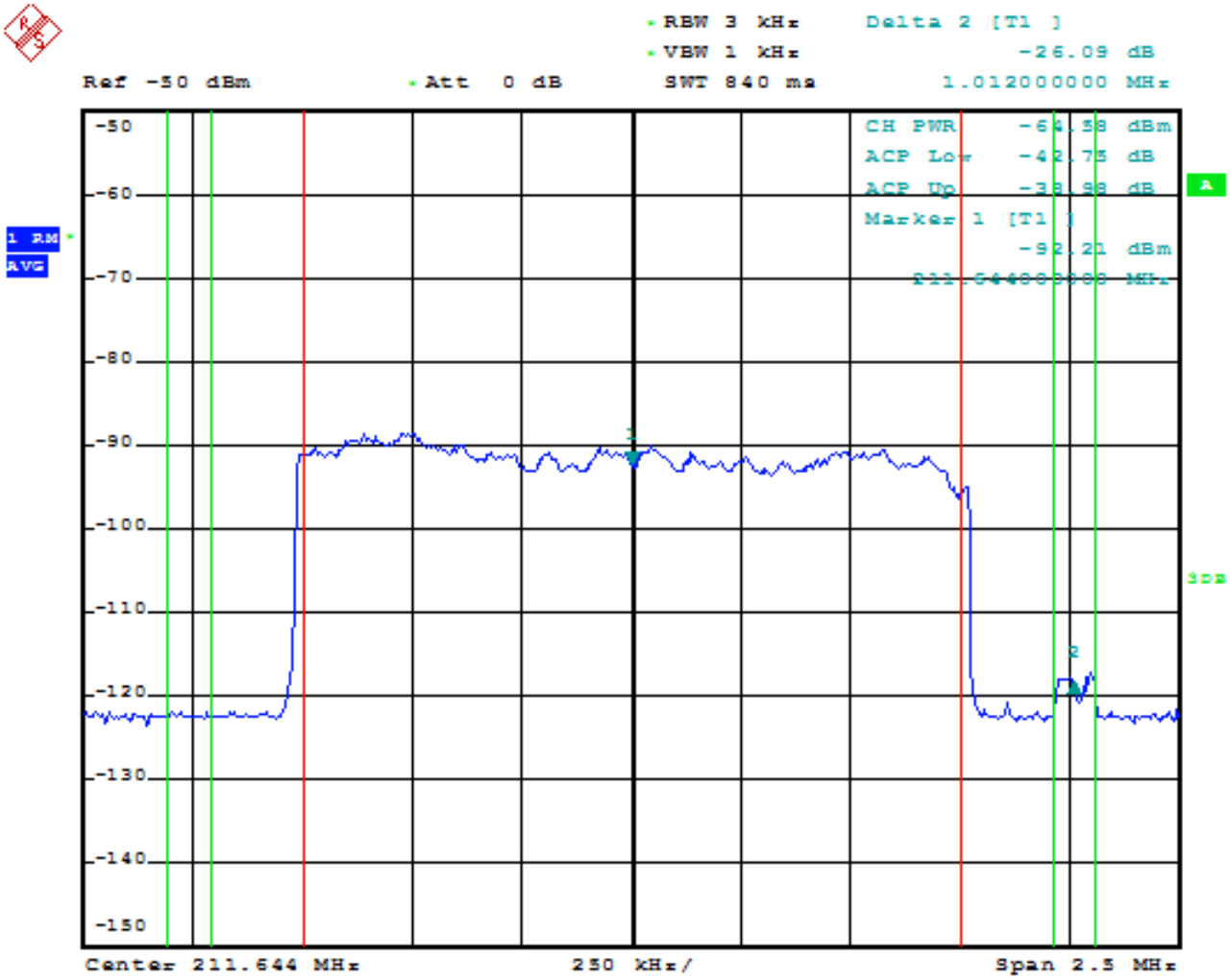

Fig. 7.3: Levels for a stationary reception scenario. Wanted: DAB, unwanted: DRM$^+$.

8 Investigation in DRM$^+$-coverage probabilities for the mobile reception scenario

The huge amount of data acquired during the measurement drives allows many more of research options than plainly documenting the coverage situation attained in the trial.

This chapter tries to deduce some coverage planning aspects related to radio network planning needed to reach a certain DRM$^+$-coverage probability for mobile reception.

For this, the strategy was as follows: from the measured data of a single measurement run the power-level at the receiver's input L' in dBm and the current bit-error-rate BER(L) was extracted. The levels were sorted in ascending order and rounded to the closest integer value, resulting in $L = [L']$. The associated current bit-error-ratios were interpreted according to definition [SSK09, Def. 8.0.1] as a random variable ber(L):

$$\mathrm{ber(L)} = \begin{cases} 1 & \text{for BER} \leq 1 \cdot 10^{-4} \\ 0 & \text{else} \end{cases} \tag{8.1}$$

After the inspection of all existent value-pairs, a point-estimation $\widehat{\mathrm{ber}}(L)$ for the 'true' bit error probability (with N(L) representing the number of all values contained in one level-bin) was performed:

$$\widehat{\mathrm{ber}}(L) \approx \frac{\sum_{n=0}^{N(L)-1} \mathrm{ber(L)}}{N(L)} \tag{8.2}$$

The mapping according to eq. (8.1) transforms the discrete random variable to a binomial distributed random variable, namely $\widehat{\mathrm{ber}}(L)$. The confidence level of this point estimation can be estimated by the method of Clopper-Pearson, since an estimation of a confidence level for a random variable with unknown probaility is involved. The confidence interval chosen is 90% due to measurement uncertainities and the simple fact that this mode of accumulation is the mode with the highest percentile score available in GRASS GIS [GRA08] when aggregating pixel values stemming from single samples (in this case: vector data in terms of a GIS) obtained from the measurement system to raster values. The evaluation is based on the raster grid used in the previous chapters. Those bins that don't contain enough samples for the estimation of the confidence interval are dropped.

The following figure 8.1 shows a measurement run that extends beyond the standard-measurement route to include the region of the B40 / Pariser Straße / Kaiserslautern Downtown and the university's living quarters. This run was made on a late noon in the march during snow conditions with 90 W in 16-QAM-mode. This certain run is the data basis for the data evaluation as depicted above using equations 8.1 and 8.2.

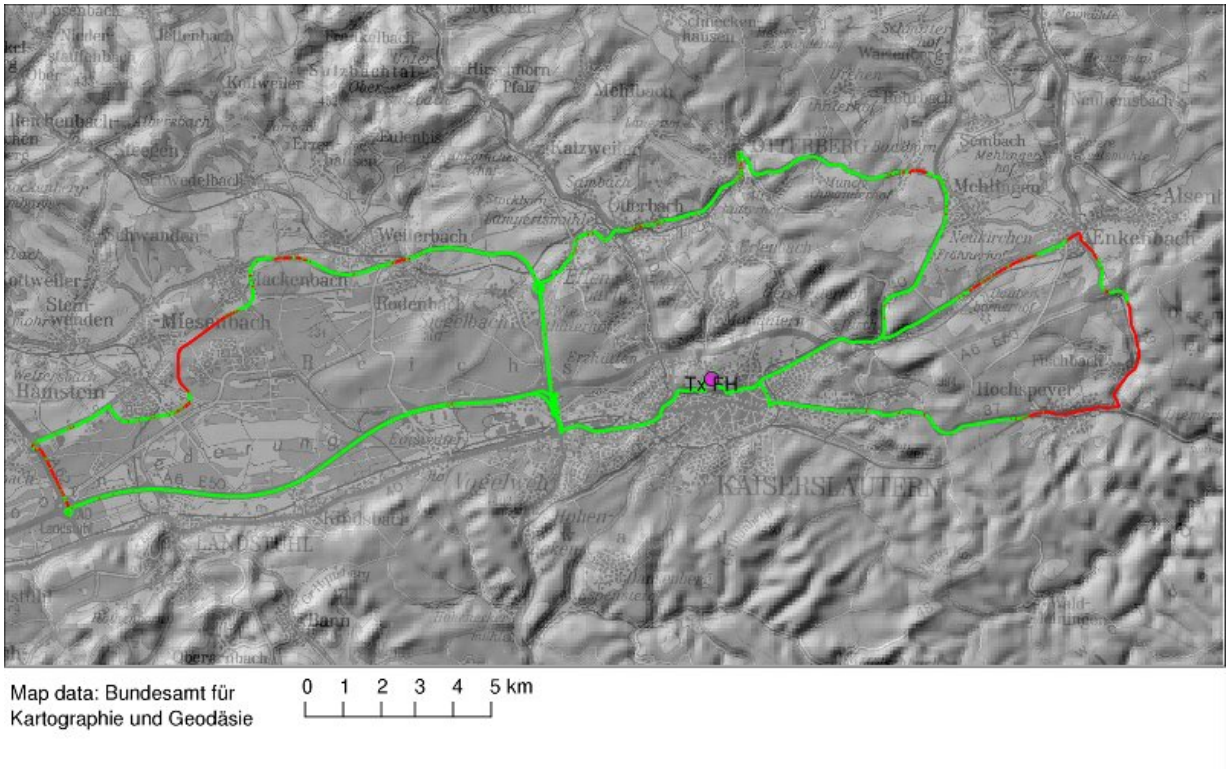

Fig. 8.1: Input route samples for fig. 8.2; the colors represent the current ber in the red/green scheme used in the figures of previous sections.

The measurement run in fig. 8.1 leads to the result shown fig. 8.2. This figure (and the ones of the same kind which are shown on the following pages) show the receiver input power level in dBm on the abcissa. The ordinate marks the estimated probability that the bit-error-rate is $\leq 1 \cdot 10^{-4}$ acc. to eq. 8.2. The (vertical) error bars mark the bounds of the estimation uncertainity, given by the chosen confidence interval. The span of the confidence interval is noted in the figure's description (on the figure's header), along the number of samples used for the data evaluation. Within this description, the number of 'relevant samples' denote the number of samples actually used, while of number of 'samples in total' denote the number of samples actually contained in the data pool. The difference – the number of discarded samples – marks the number of samples dropped because not enough data for a valid estimation was acquired. The figure's interior focusses on the the probabilities between 0.9 and 1.0 to enhance the readability.
An exemplary interpretation of this figure is: if a DRM$^+$-receiver is subjected to an input power level of -91 dBm along a random spot of the measurement route, then there is a chance of 50% that the received frame yields a BER $\leq 1 \cdot 10^{-4}$. Since the figure's content is based on more samples in more regions than just the standard measurement route, chances are not that bad that those 50% will also result in other places of the route – as long as the condition 'input level is -91 dBm' is fulfilled.
Another way of reading those figures is: emanating from the receiver input level where the median (the 50%-value) of $\widehat{\text{ber}}(L)$ is reached, the additional transmitter power can be read out from the graph to reach a certain coverage goal for the momentary bit error ratio along the measurement route where the condition BER $\leq 1 \cdot 10^{-4}$ is met. Starting at the value of -91 dBm, where the P(BER) $\leq 1 \cdot 10^{-4} \approx 0.5$ is met first, an additional receiver input power of 8 dB is needed to reach a probability of P(BER) $\leq 1 \cdot 10^{-4} \geq 0.99$, when the uncertainity given by the confidence interval is taken into account.

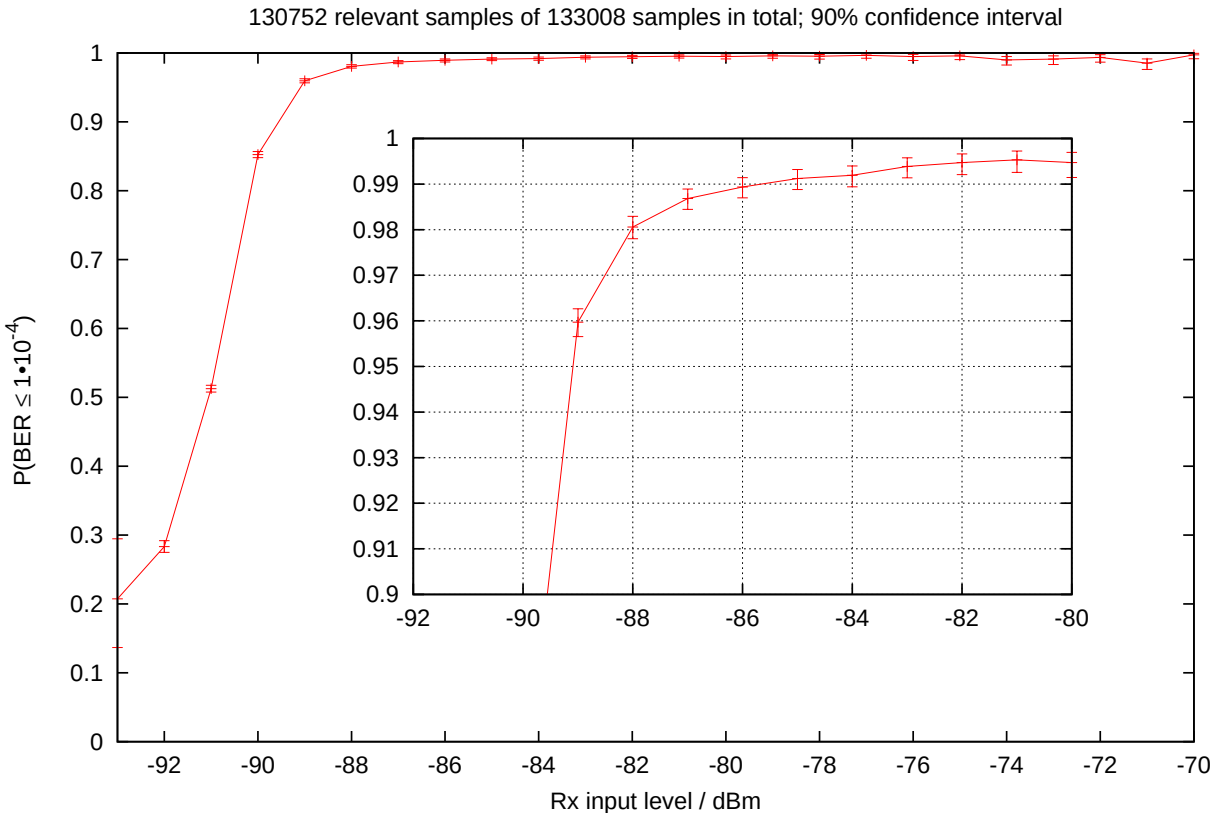

Fig. 8.2: Evaluation of coverage-probabilities for mobile reception, 16-QAM, Winter 2009. EIRP: 90 W

This evaluation strategy was repeated for a test run along the standard measurement route in the 16-QAM-mode with a radiated power of 180 W during the summer. The result is shown if fig. 8.3. Due to the minor amount of samples (remember the route deviations!), less valid values can be used for the plot. This essentialy leads to larger error bars than in fig. 8.2. Repeating the interpretation noted in the paragraph above to derive the planning additions from 50% to 99% makes the value of 8 dB show up again, supporting the statement from the previous paragraph.

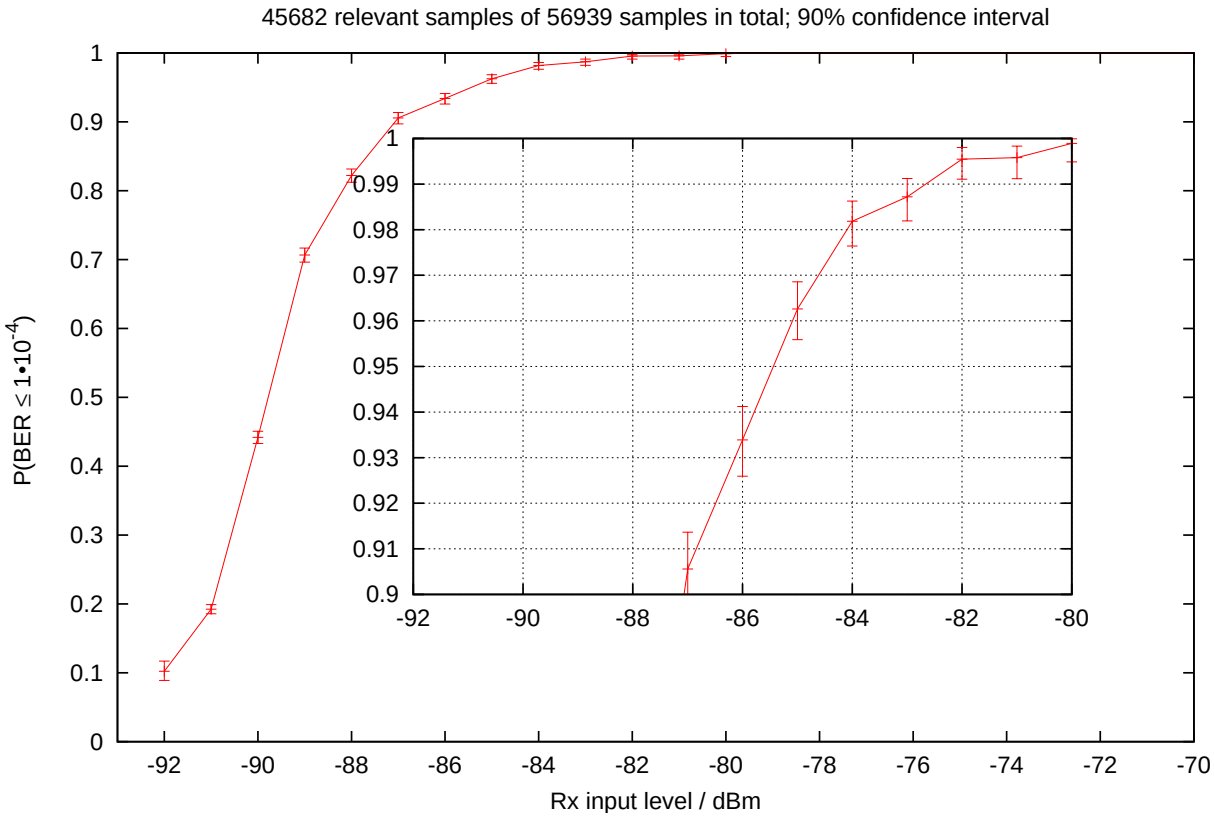

Fig. 8.3: Evaluation of coverage-probabilities for mobile reception, 16-QAM, Summer 2010. EIRP: 180 W

Comparing fig. 8.2 and 8.3 shows

- a shift in power levels: in the winter phase, less input power is needed to reach a certain percentage, which mainly stems from the rise in transmit power. It is to note that a general level uncertainity of ±1 dB has to be assumed for the spectrum analyzer used for level measurement.
- a different gradient in the percentage region of 0.9 . . . 1.0. This might be misleading due to less samples in total resp. for each single bin and the high steepnes / sensitivity in this percentage region.
- that the power offset needed to rise the coverage probability from e.g. 50% to 99% is 8 dB in both cases. Except from the uncertainities noted in the two points above, there is no other change in the basic setup of this experiment. Since the chance of sucessful decoding is substantially a function of the received carrier to noise ratio, the transmitter's EIRP's aren't of interest here.

Evaluating the coverage situation in the field in the 4-QAM-mode during the summer with a radiated power of 180 W leads to fig. 8.4. It is evident that the median is reached earlier (for lower input levels) and, as expected, the decoding chance's gradient is steeper as compared to the 16-QAM-variant: the transistion from $P(BER) \leq 1 \cdot 10^{-4} \approx 0.5$ to $P(BER) \leq 1 \cdot 10^{-4} \approx 0.99$ is roughly only about 3 dB.

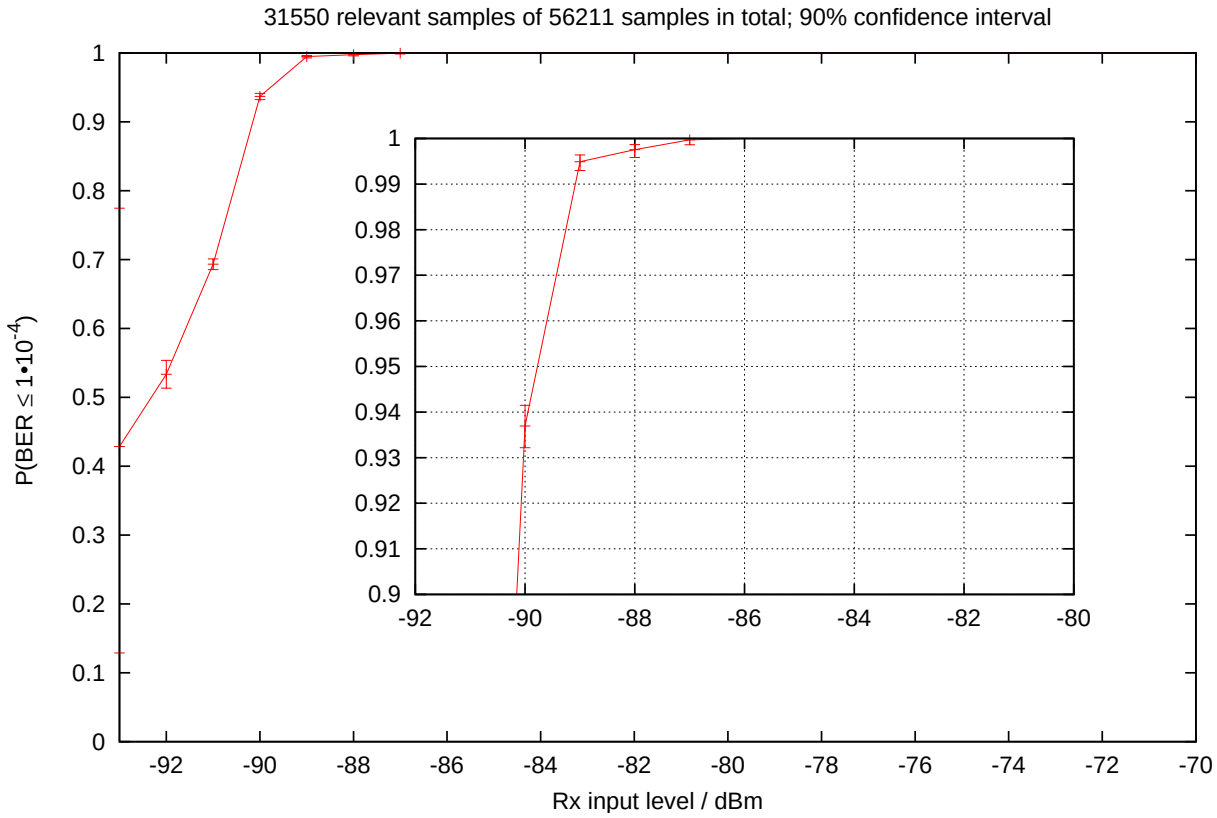

Fig. 8.4: Evaluation of coverage-probabilities for mobile reception, 4-QAM, Summer 2010. EIRP: 180 W

The derivation up to this point opens the possibility to check those assumptions. As noted before, the prediction's threshold is the probability-bound of 90%. For this, the measured samples in 16-QAM-mode (no interference) are inspected. If the level of a single sample is at least −89 dBm (representing the 90%-margin), then it is marked good, bad otherwards. Afterwards, the samples are resampled to a raster grid of 100 × 100 m. The resampling method is the 90th percentile, thus: the value representing the 90th percentile obtained from all samples contained in the region of a grid cell is the output value for plotting and for further use. The result is shown in fig. 8.5.
In the next step, the data represented by fig. 8.5 was compared to the measured result shown in fig. 8.6, resulting in fig. 8.7. 9.5% of the raster cells show a mismatch between prediction and measurement, which means that – vice versa – 90.5% of the raster cells that were taken into account for the prediction 'hit the spot'. The predicted hits just don't match to those raster cells where there just hasn't been any reception at all – they even include *and follow* those route sections where reception conditions were at the edge between 'ok' and 'fail'.

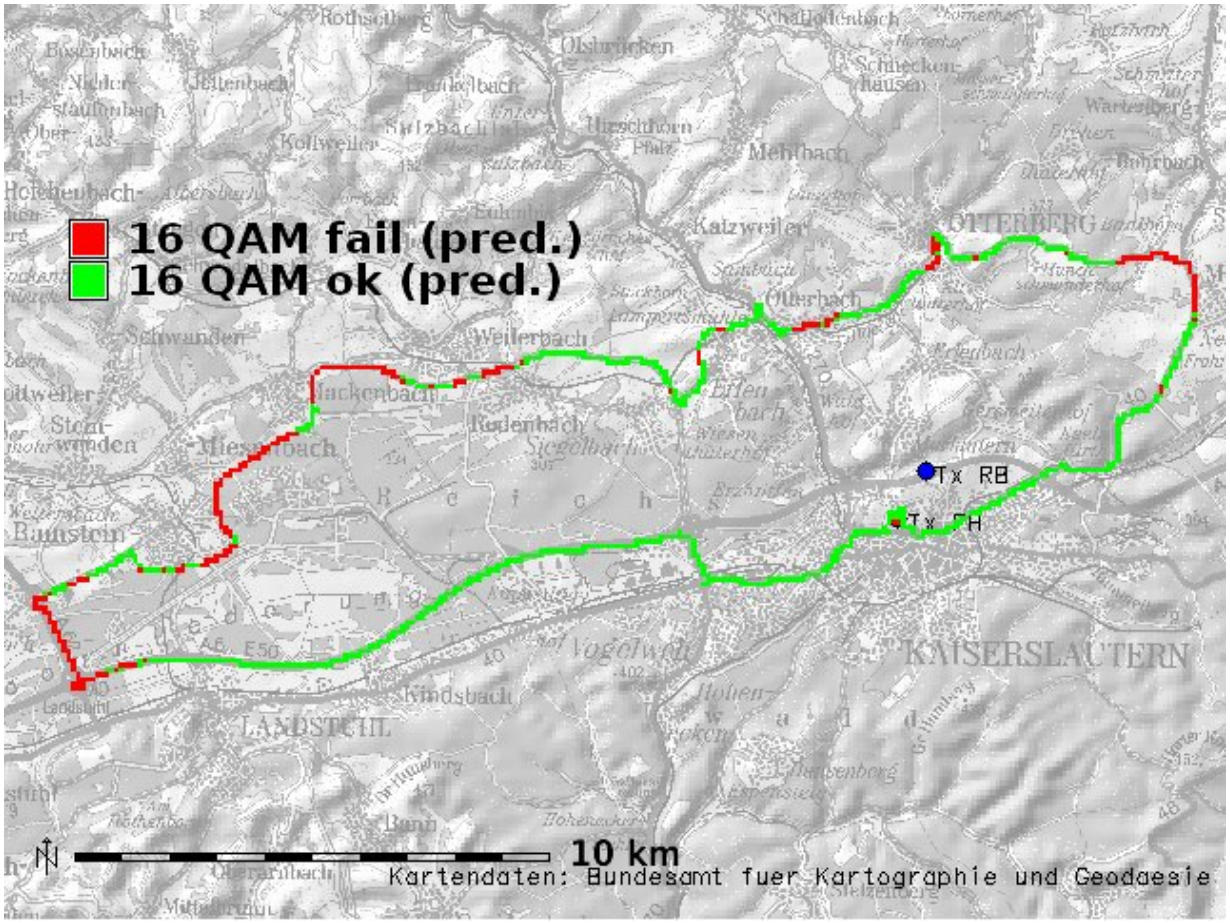

Fig. 8.5: Predicted coverage with a coverage probability of 90% using the data gained in this chapter, along with measured receiver input power data when TX FH operates at 90 W

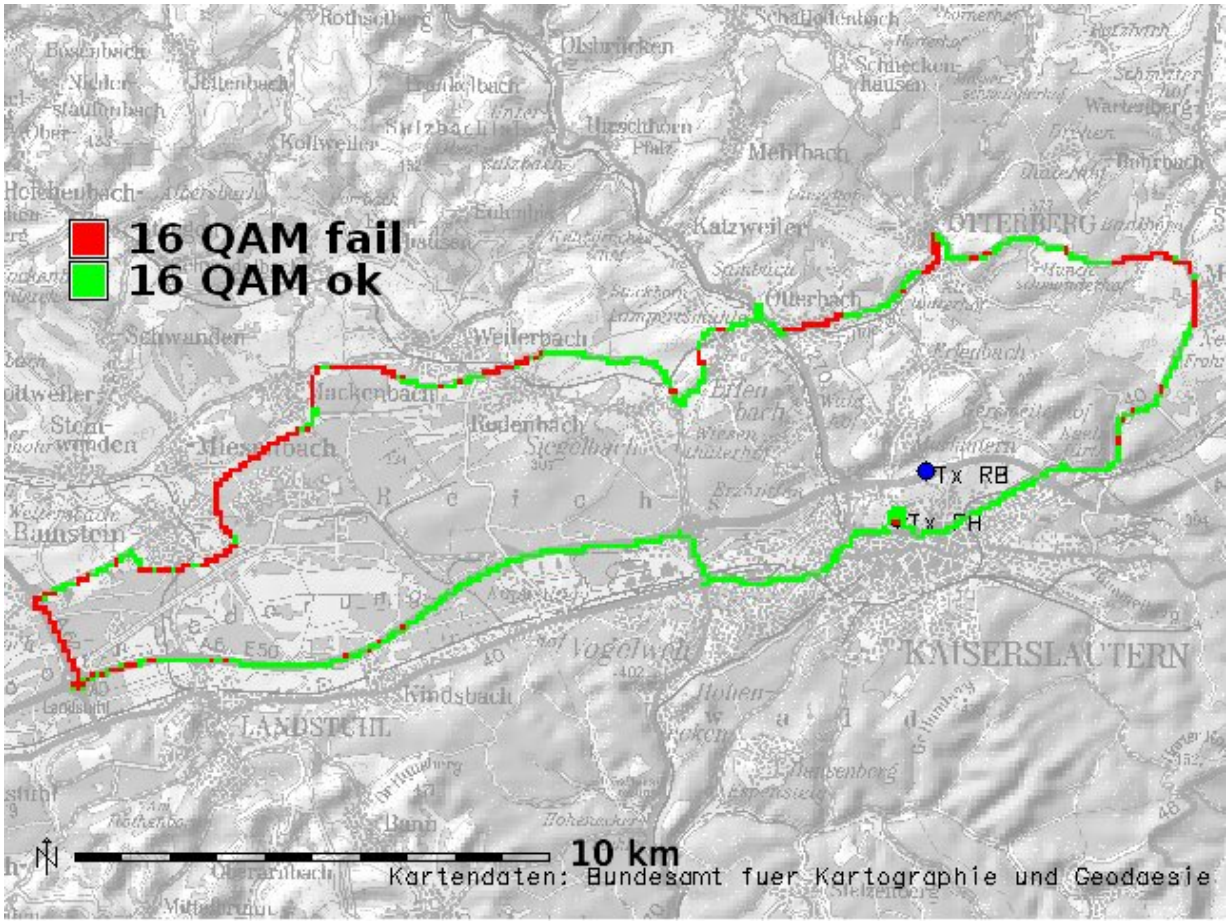

Fig. 8.6: Measured coverage (90 W ERP, 16-QAM MSC-modulation)

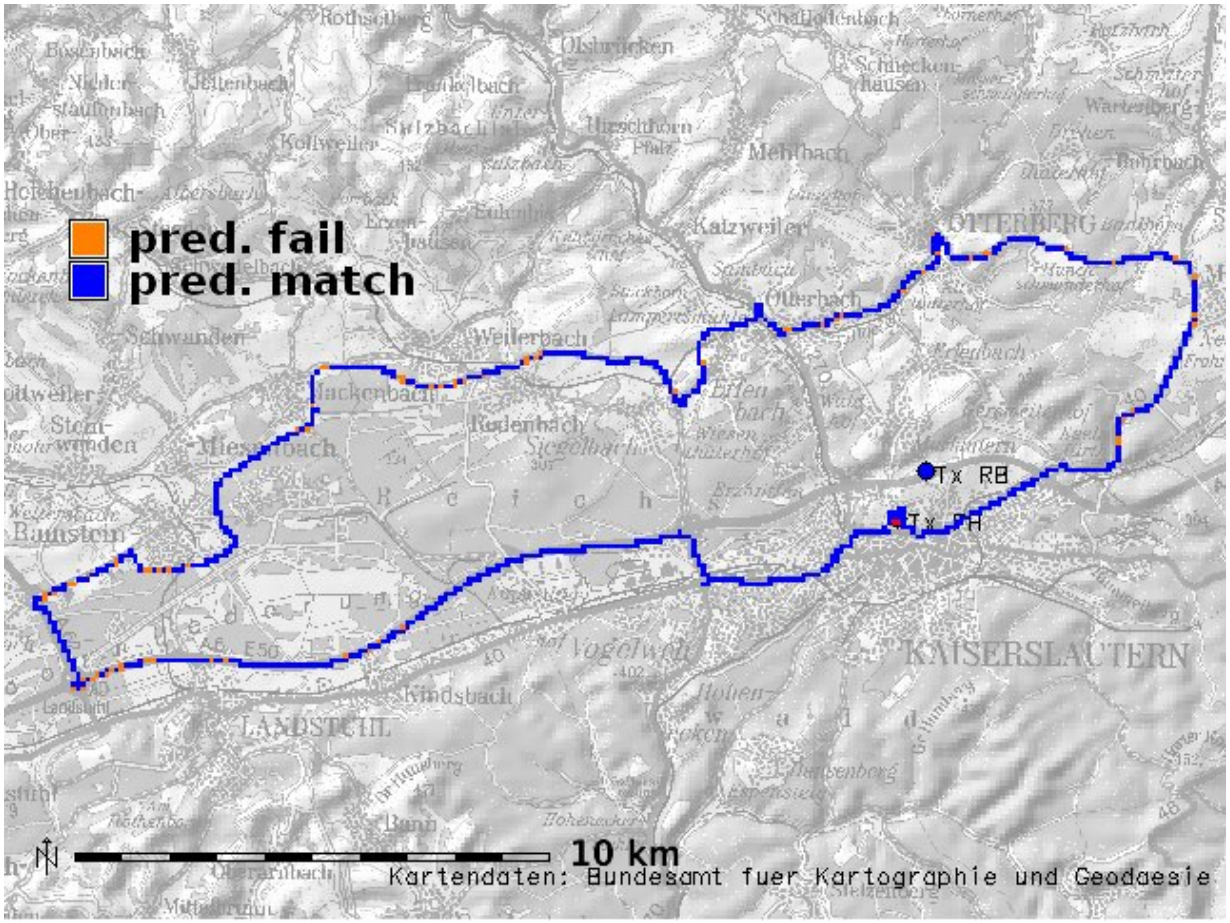

Fig. 8.7: Comparison of measured and predicted coverage on the base of the two previous fígures

It is evident to note that – as emphasized before – the results are only valid for the local situation and geographical circumstances. The surrounding enviroment profile fits at best into the category 'hilly terrain' / 'suburban area' (suburban due to the size and building architecture predominant in Kaiserslautern). Furthermore, using the data given in this report and [Köh10], a mapping of the receiver input levels to a carrier to noise ratio could be possible. Furthermore, it should be noted that the coverage supplements given here describe the location's variance (speaking in terms of fieldstrength prediction), although part of the time variance is included due to the differences in the seasons where the measurements had been taken.

As demonstrated in the previous paragraphs, the method shown leads to results that seem to enable a quite realistic estimate of the coverage obtainable by an DRM$^+$-transmitter operated on Band III. The figures following represent the same set of measurement data as shown before. In contrast to those figures above, a confidence interval of 95% was chosen to get a tigther estimate of the coverage supplementes (leading to larger error bars). Furthermore, the separation betweeen summer and winter data is kept to allow a comparision regarding the probabilities change due to the variance of time.

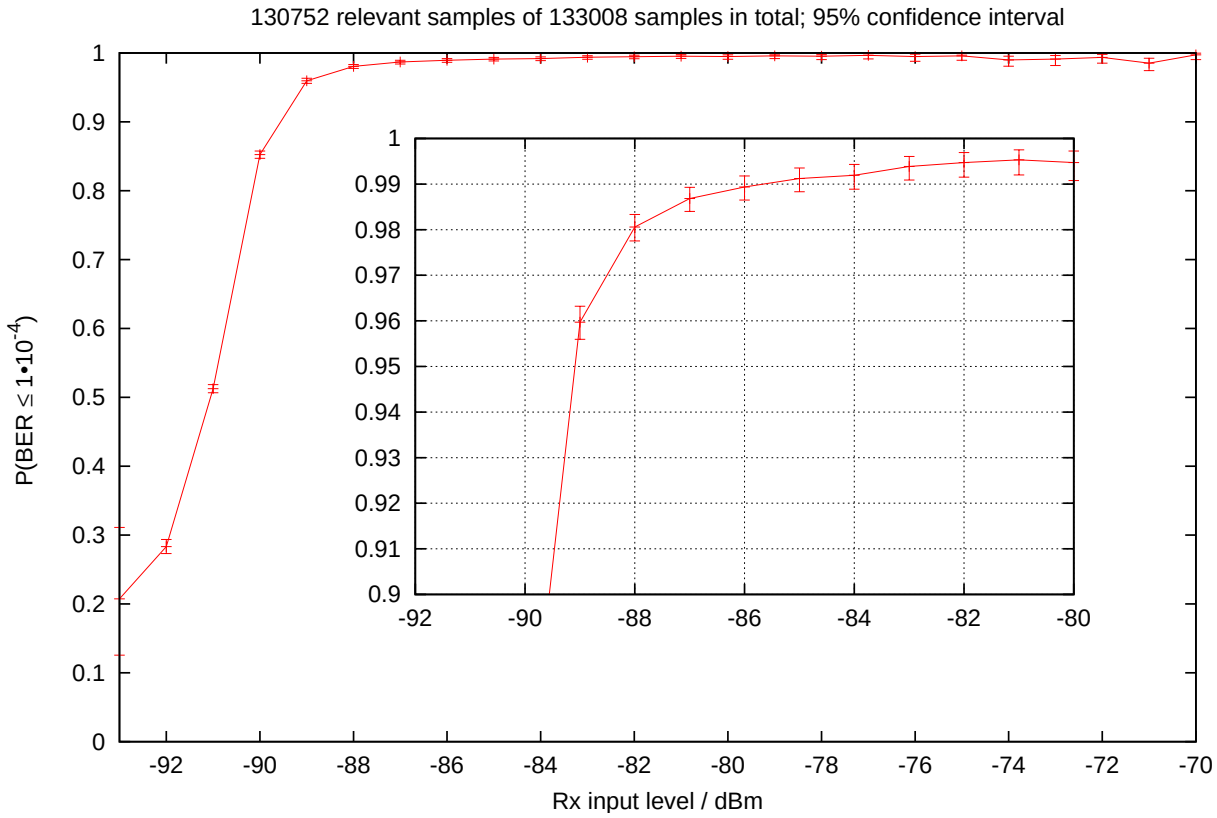

Fig. 8.8: Evaluation of coverage-probabilities for mobile reception, 16-QAM, Winter 2009. EIRP: 90 W

The figure above (fig. 8.8) shows the measurement data set for a 16-QAM-run during the winter with an EIRP of 90 W, cf. fig. 8.2. The confidence interval for the probability estimation has been set to 95%. It can be seen that the step from 50%-coverage probability to a 99%-coverage probability is 8 dB, just like for the 90%-evaluation.

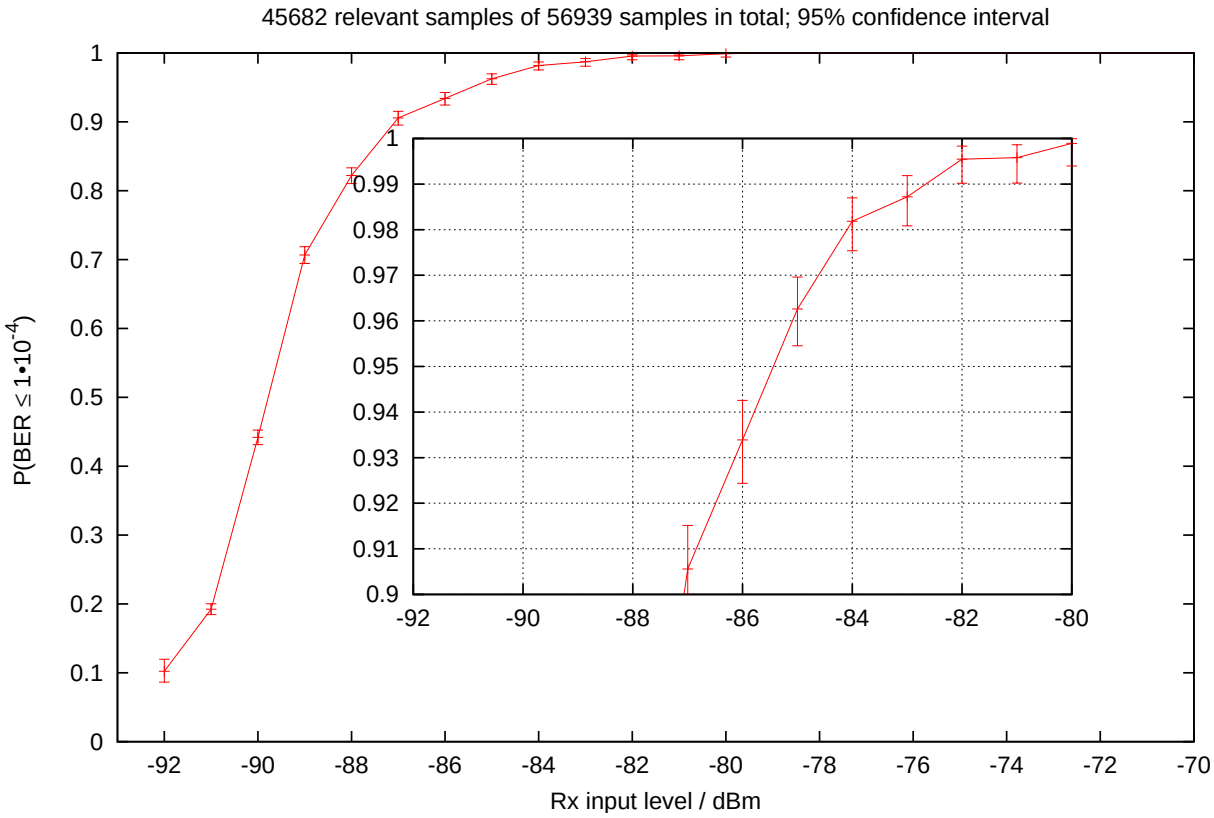

Fig. 8.9: Evaluation of coverage-probabilities for mobile reception, 16-QAM, Summer 2010. EIRP: 180 W

The figure above (fig. 8.9) shows the measurement data set for a 16-QAM-run during the summer with an EIRP of 180 W, cf. fig. 8.3. The confidence interval for the probability estimation has been set to 95%. It can be seen that the step from 50%-coverage probability to a 99%-coverage probability is 8 dB, just like for the 90%-evaluation and the previous results.

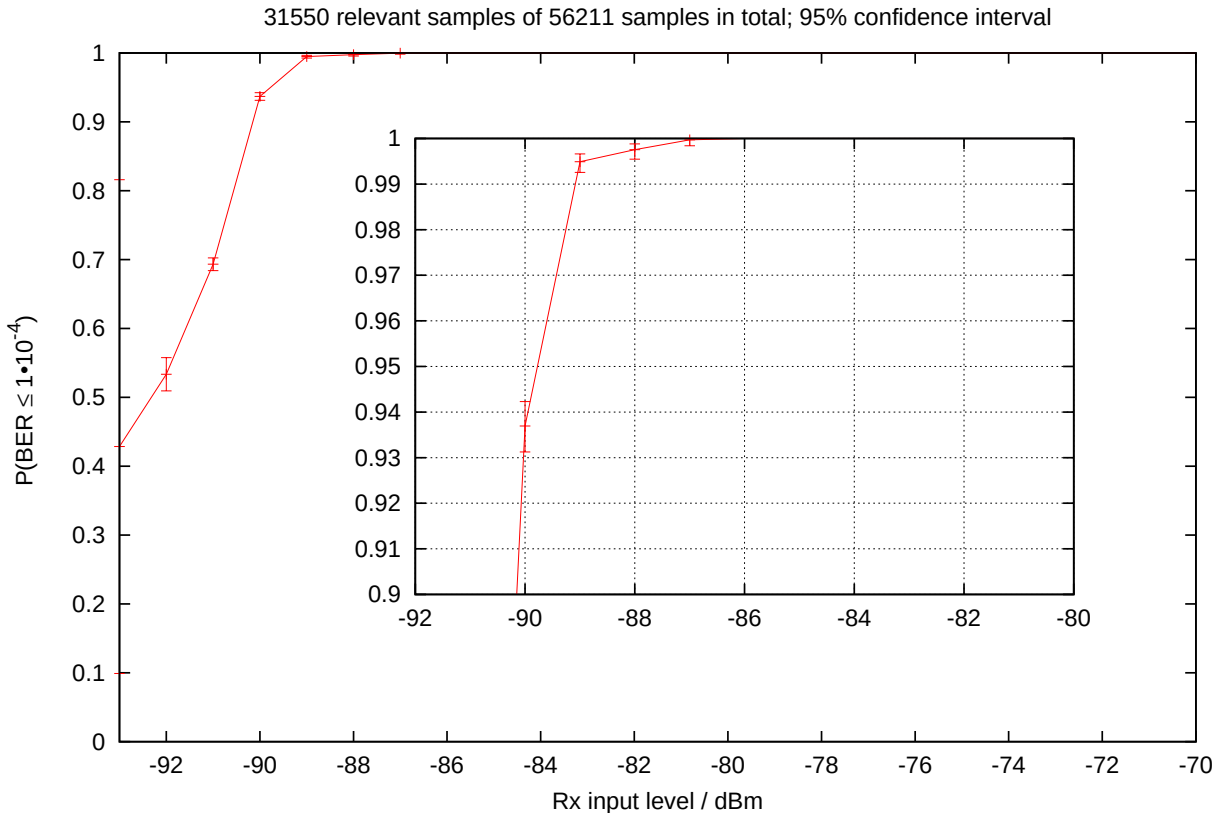

Fig. 8.10: Evaluation of coverage-probabilities for mobile reception, 4-QAM, Summer 2010. EIRP: 180 W

The figure above (fig. 8.10) shows the measurement data set for a 4-QAM-run during the summer with an EIRP of 180 W, cf. fig. 8.4. The confidence interval for the probability estimation has been set to 95%. It can be seen that the step from 50%-coverage probability to a 99%-coverage probability is 3 dB, just like for the 90%-evaluation.
For both cases of the MSC-modulation-modes (16- or 4-QAM), the required offset from a 50%-coverage probability for a mobile reception scenario tends to be in the range of 8 dB (16-QAM) resp. 3 dB (4-QAM), regardless of transmission power and season within a 95% interval of confidence. The validity for this derivation has been shown by the transfer of the results gained from an extended measurement run to the results gained from the standard measurement route. A comparison between measured and predicted results along the measurement route has shown a good chance of correct results within the investigated planning raster's grid size of 100×100 m under the consideration of the confidence interval.

9 Some notes about speed issues for DRM$^+$ operated in Band III

The speed of a mobile DRM$^+$-receiver is far more limited when the system is operated in Band III as compared to VHF-Band II. A first insight into the limitations is shown in [Köh09], whereas speeds over 150 km/h (16-QAM-mode) are barely achieved for the simulation profiles given there, assuming a center frequency of 230 MHz.

During the measurement runs, the top speed given by the measurement system was limited to 120 km/h. During those route's sections (provided sufficent receiver input power was available, i.e. in highway sections at the border of Kaiserslautern), no reception failures were recorded as can be seen from the figures in the previous chapters. In the western section of the test route, the speed is limited to 130 km/h. Test runs in this region at the given speed limit showed no reception failures due to those doppler issues.

To get a further impression of the doppler performance for DRM$^+$ in this frequency range, a drive test with the Fraunhofer IIS's demo car was initiated spontaneously. No suitable recording facility could be established due to the lack of time, thus the impressions gained can be only expressed by words.

The setup was as follows during the 3rd phase: TX FH was operated at 180 W in 4-QAM-mode with TX RB switched off. The demo vehicle was equiped with an $\lambda/4$-dipole with a magnetic mount on top of the demo limousine. Rx1 was packed into the limousine's trunk, along with a modified power supply. The decoding and monitoring laptop was set up in the rear seat of the vehicle; the audio lines from the decoder's output were connected to the car's audio system. An independent GPS-receiver was used to track the vehicle's position and speed.

The following figure 9.1[1] depicts the driven path. The transmitter site of TX FH is indicated by a brown triangle; the path's color indicates the speed range in km/h. The test route led to the cities western part until the higway-crossing of Landstuhl (not shown on the map). In this section, only speed of max. 130 km/h is allowed. It could be confirmed that reception conditions were stable as seen in the measurement runs with the van used previously during this drive and along the cities inner sections. Afterwards, the motorway A63 Kaiserslautern - Mainz leading to the north-east was chosen. The fieldstrength in this area is lower due to terrain obstructions, but nonetheless, LOS conditions are slightly better on the motorway esp. in the region of Mehlingen / Sembach as compared to countryside-road chosen for the measurement route used in the previous test runs due to a higher elevation. Furthermore, the speed is partially off-limits in this section of the street. The fact that the coverage from TX FH in this region is not quite good led to the decision for the 4-QAM-mode for it's relaxed S/N requirements. This way, reception was possible up to the vicinity to Rohrbach, which was tested on the way outwards to Lohnsfeld. On the way back (onward to the transmitter site), several accelerations and decellerations in the range of 200 ... 220 km/h showed that audio decoding failed at roughly 210 km/h. Unfortunately, a direct comparison with the evaluations in [Köh10, chap. 4.2.3] is not possible due to the different MSC-decoding scheme, the lower center frequency of the DRM$^+$-multiplex and the fact that the terrain's profile can't be compared to the path profiles used for the simulations, esp. when the short route driven (not lots of samples in a statistical sense) is considered.

[1] Please note that the motorway A63 isn't drawn on the map, for the map is slightly out of date.

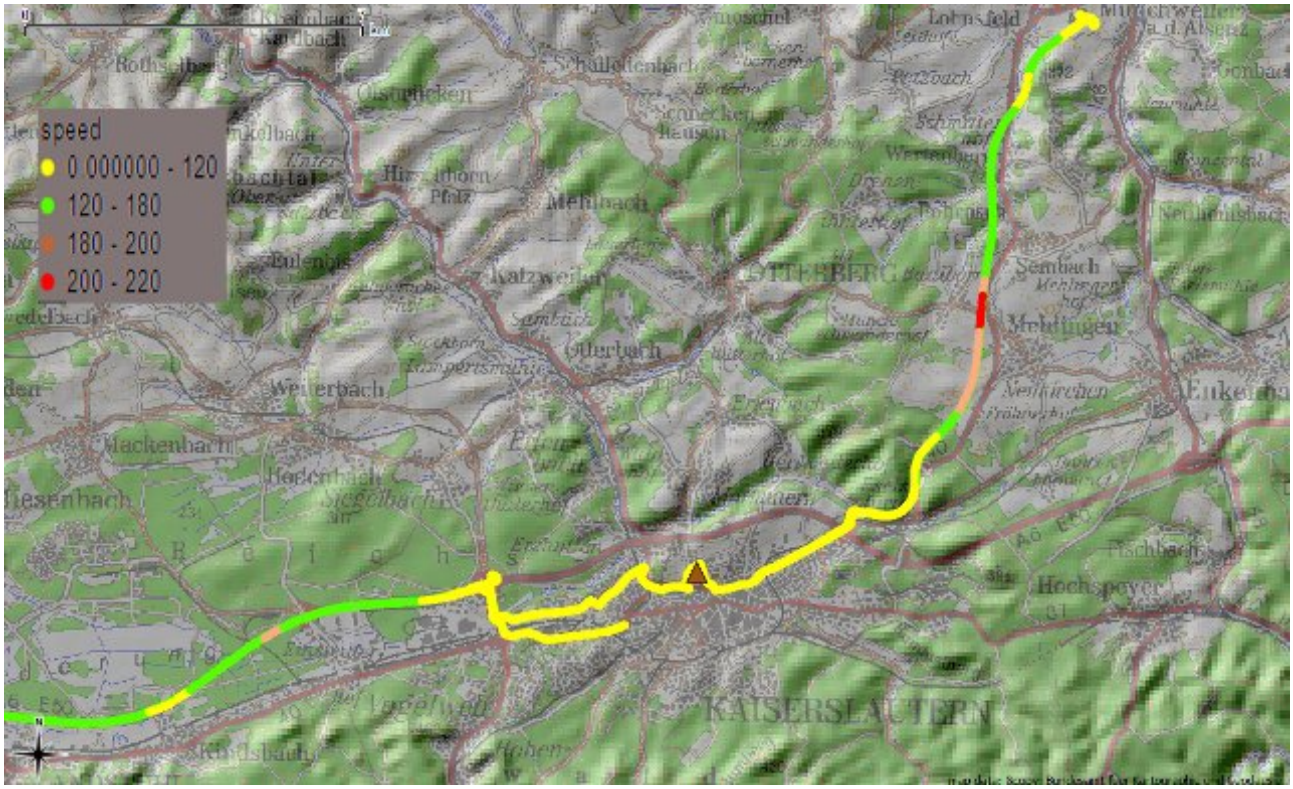

Fig. 9.1: Drive test path. Colors mark the speed range in km/h; TX FH is marked by a brown triangle

10 Final conclusions

The field trial described in this report at hand has shown that the operation of DRM$^+$ in the VHF Band III is possible in a real-world scenario.

Regarding the adjacent and co-channel interference scenarios dealt with during the trial, the system's performance in the field tends to match up with the protection ratios worked out in [Köh10]. This also holds when not only mobile reception, but also a stationary reception scenario is taken into account. Furthermore, the transmitter's coverage tends to meet the coverage areas estimated by frequency planning esp. if the receiver's sensitivity is regarded.

Furthermore, some insights could be gained into the system's performance due to doppler shifts in this frequency range. Experiments show that this issue might not be that crucial for real world applications (except high speed trains), esp. when the lower frequency blocks in this frequency range could be used.

In a next step, the compatibility of DRM$^+$ into services adjacent to the VHF Band III should be elaborated to harden the system's option for it's succesful establishement in this frequency range.

Bibliography

[Ber05] Bernhardt, Frank: *Untersuchung zur Implementierung eines digitalen Übertragungssystems auf OFDM-Basis im UKW-Frequenzbereich*, Fachhochschule Kaiserslautern, Diplomarbeit, November 2005

[Fei05] Feilen, Michael: *Objektorientierte Implementierung eines Sendesystems für Digital Radio Mondiale*, Fachhochschule Kaiserslautern, Diplomarbeit, Oktober 2005

[GRA08] GRASS Development Team ; Open Source Geospatial Foundation (Hrsg.): *Geographic Resources Analysis Support System (GRASS GIS) Software*. Open Source Geospatial Foundation, 2008. `http://grass.osgeo.org`

[HSE07] Hasenpusch, Th. ; Schad, F. ; Effinger, R.: Compatibility Measurements: DRM120, DRM+ and HD-Radio^{TM} interfering with FM Broadcast, Narrowband FM (BOS) and Aeronautical Radionavigation / Federal Network Agency of Germany and Fachhochschule Kaiserslautern. 2007 (G531/00328/07)

[Ins09] Institute, European Broadcasting Union & European Telecommunications S. ; European Telecommunications Standards Institute (Hrsg.): *ETSI ES 201 980 – Digital Radio Mondiale (DRM): System Specification*. V3.1.1. 650 Route des Lucioles,F-06921 Sophia Antipolis Cedex – FRANCE: European Telecommunications Standards Institute, Februar 2009

[Köh09] Köhler, Martin: Performanceuntersuchung von DRM^{+}Decoder Prototypen / FH Kaiserslautern. 2009

[Köh10] Köhler, Martin: *Messtechnische Bewertung der Nutzbarkeit von DRM^{+} im VHF-Band III*, Fachhochschule Kaiserslautern, Diplomarbeit, April 2010

[Lee93] Lee, William C. Y.: *Mobile communications design fundamentals*. 2nd ed. Wiley-Interscience, 1993. – ISBN 0–471–57446–5

[Mic] Microtelecom S.r.l.: Perseus SDR Homepage. `http://microtelecom.it/perseus/`

[Sch07] Schad, Felix: *Generierung und Mischung von DRM-Signalen zur Senderansteuerung*, Fachhochschule Kaiserslautern, Diplomarbeit, 2007

[SLSK08] Steil ; Lehnert ; Schad ; Köhler: Leaving the dead-end street: New ways for the digitisation of the VHF-FM sound broadcasting with DRM^{+}. Pt. III: Outlook: Investigations ojn the deployment of DRM^{+}in Band III. In: *9th Workshop Digital Broadcasting* Fraunhofer Gesellschaft für Integrierte Schaltungen (IIS), 2008

[SS08] Schad, F. ; Steil, A.: Abschlussbericht zum DRM^{+}-Feldversuch Kaiserslautern. Versuchszeitraum: 1. März 2008 – 31. Mai 2008 / Fachhochschule Kaiserslautern, LMK Rheinland-Pfalz. 2008

[SSK09] Schad, F. ; Steil, A. ; Köhler, M.: Abschlussbericht zum DRM^{+}-Feldversuch Kaiserslautern. Versuchszeitraum: Januar – August 2009 / Fachhochschule Kaiserslautern, LMK Rheinland-Pfalz. 2009

List of Figures

List of Tables